

The importance of hydrodynamics on the initiation of thermoacoustic oscillations: Transient and Limit Cycle Thermoacoustic Oscillation Dynamics in a Lean Premixed Swirl Stabilized Combustor

Efstathios Karlis, Yannis Hardalupas, Alex M.K.P. Taylor

Mechanical Engineering Department

Workshop on Analytical methods in thermo- and aero- acoustics

University of Keele

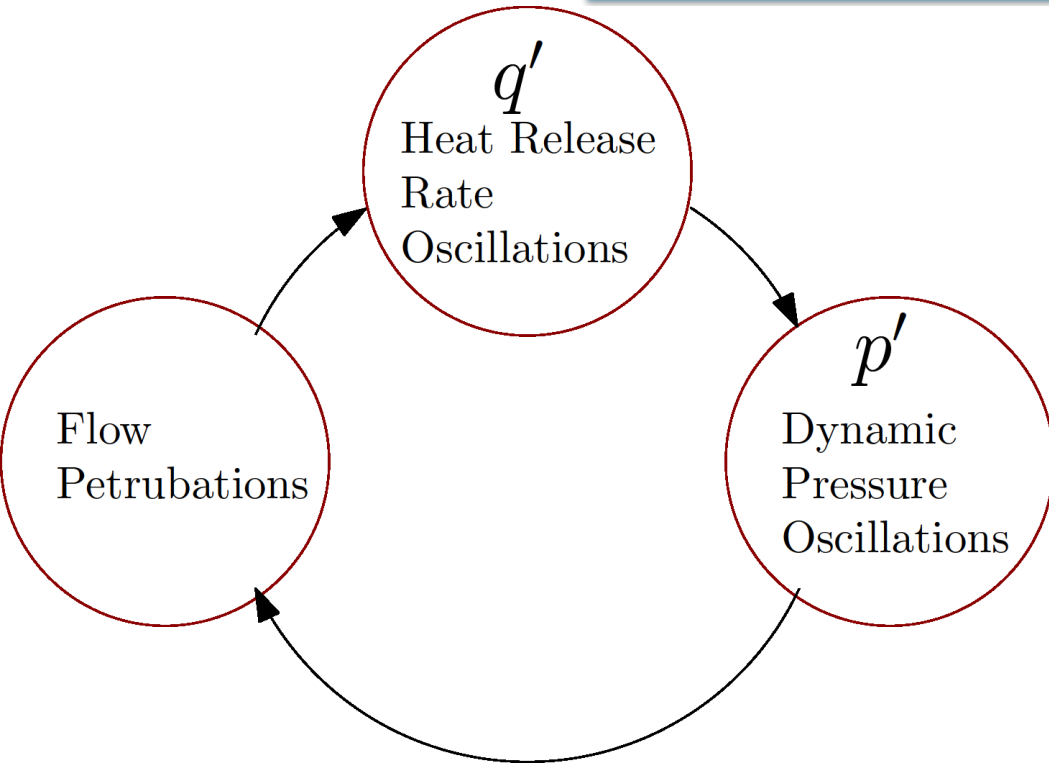
11 March 2020

- Introduction to Thermoacoustic instabilities – Link to Rayleigh Criterion
- Experimental approach used for the physical understanding of the problem
- Interpretation of what triggers the Thermoacoustic instabilities
- Interpretation of how Thermoacoustic instabilities perpetuate

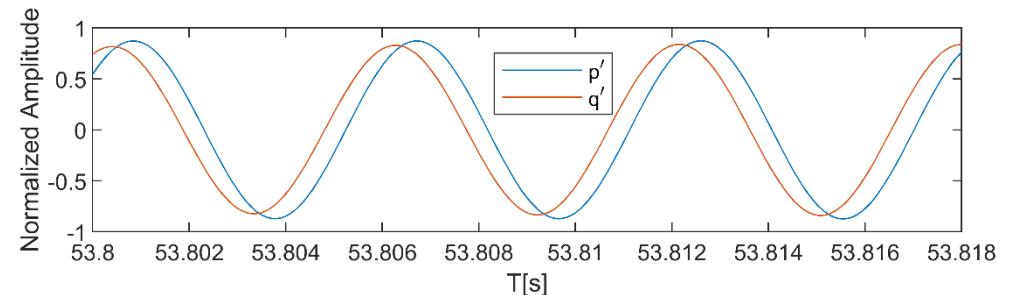
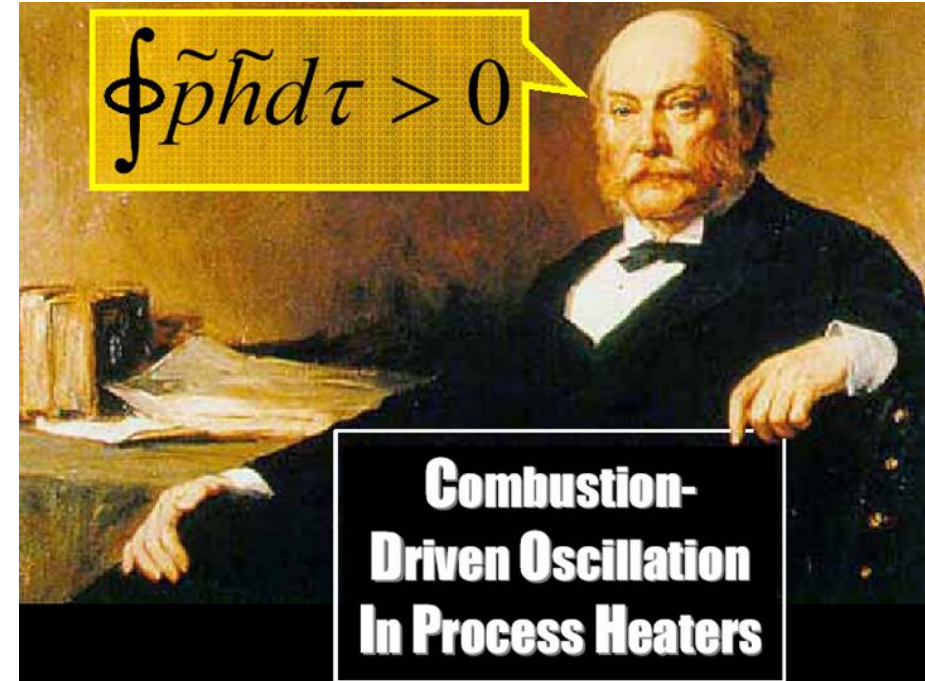


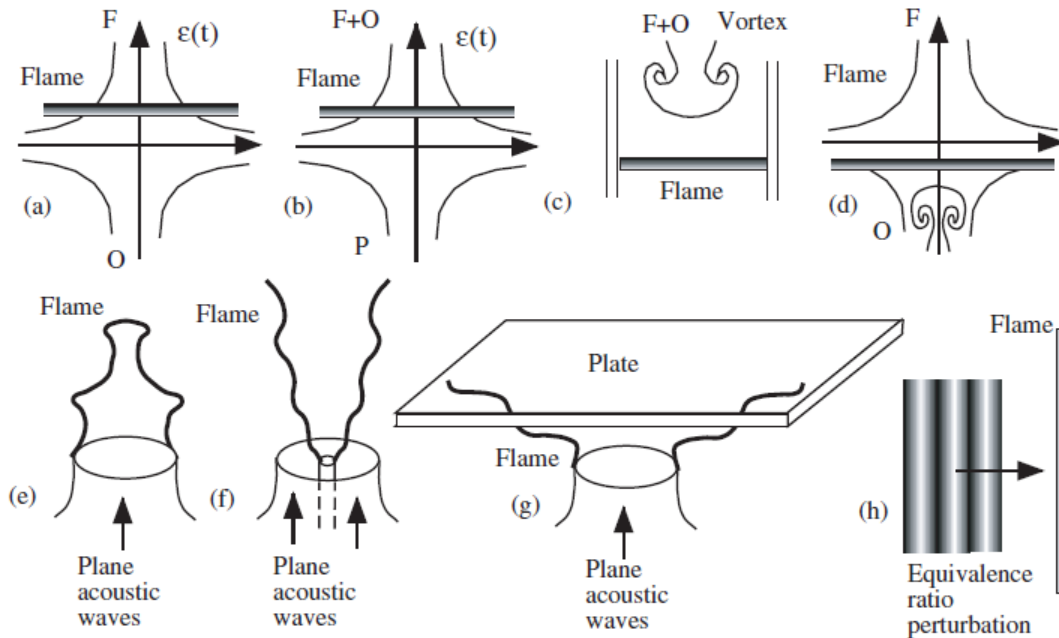
Burner assembly damaged by combustion instabilities (left). New assembly (right). Goy et al. 2005

- The lean premixed mode of operation is employed for land-based Gas Turbine power generation in order to reduce NO_x emissions.
- Unfortunately the lean premixed mode of operation makes combustors susceptible to the triggering of combustion instabilities, in the form of thermoacoustic oscillations.



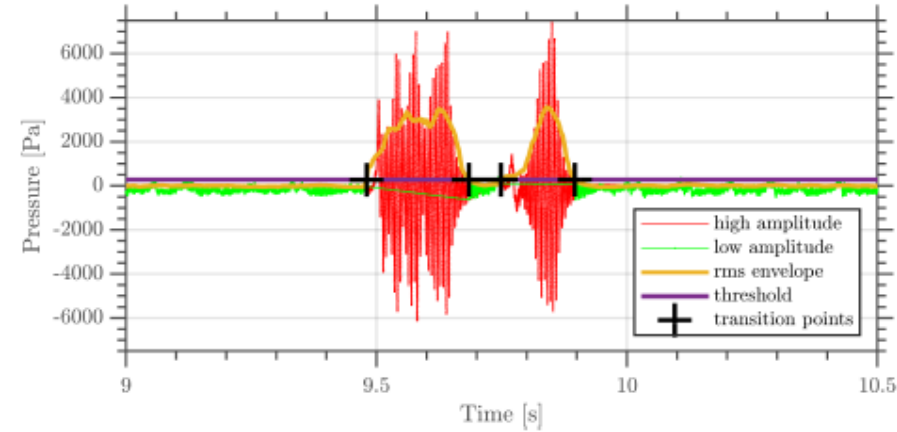
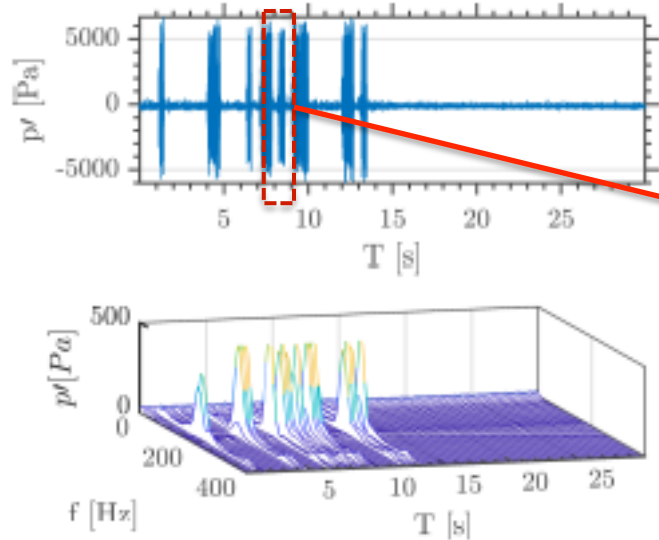
Rayleigh criterion: Perpetuation of thermoacoustic oscillations if p' and q' oscillate in phase





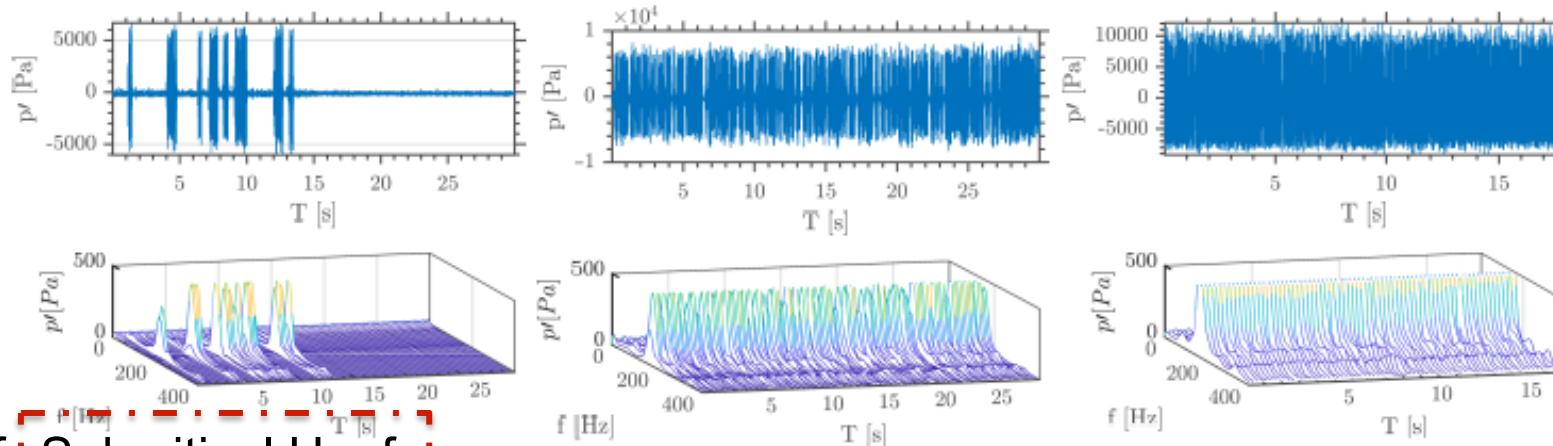
Thermoacoustic mechanisms (right). Candel et al. 2002, Proceedings of the Combustion Institute

- Perpetuation mechanisms are still under investigation but in essence are described by the Rayleigh criterion.
- Mechanisms in elementary combustors include: Vortex-Flame interactions, Equivalence ratio oscillations, Oscillatory Flame Stretching and others.
- Still the understanding of the perpetuation mechanisms in complex systems are not fully understood. Further investigation is required.



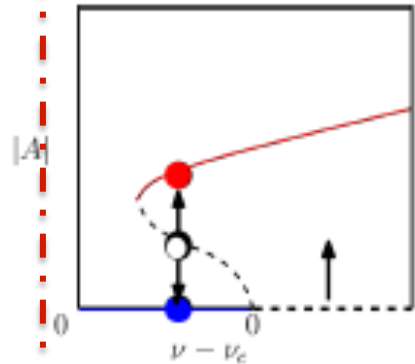
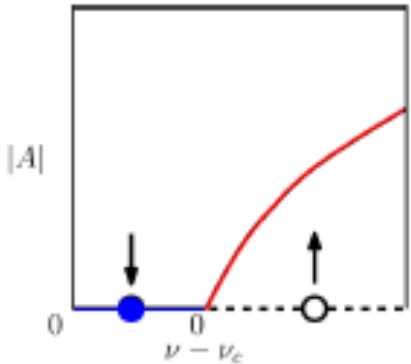
- The Rayleigh criterion does not examine what causes the combustor to become thermoacoustically unstable in the first place.
- The physics of the triggering mechanisms are even less well understood.
- It is important that these mechanisms are investigated because transitions to instabilities happen abruptly, with no prior forewarning: Subcritical Hopf Bifurcations.

Bifurcation parameters: Increasing any of ϕ , χ_{H_2} , $T_{preheat}$ etc. probability of triggering increases



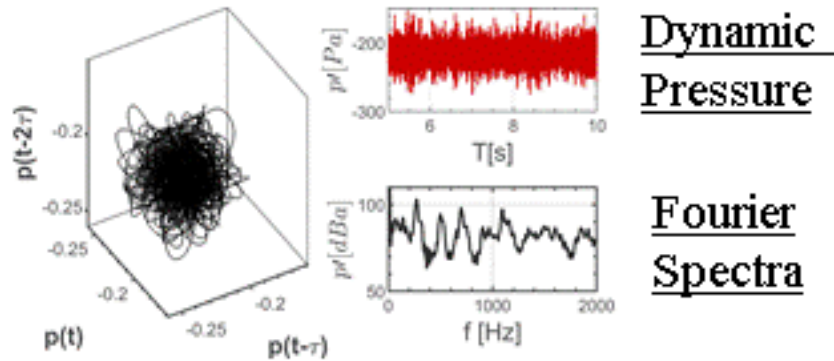
Supercritical Hopf

Subcritical Hopf



Bistability: Intermittent transition from broadband low amplitude dynamics to deterministic oscillations.

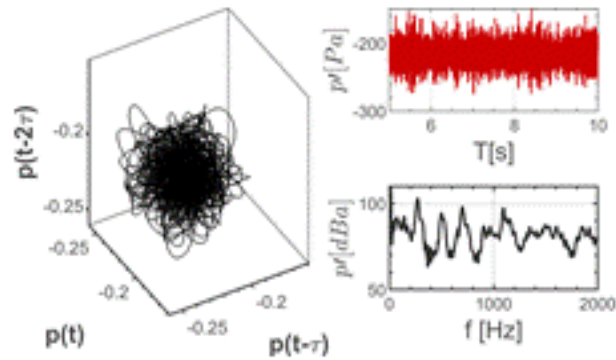
Quiescence



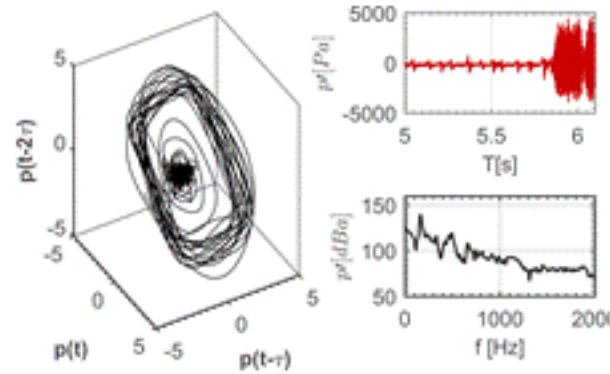
Dynamics: Attracted to fixed point and demonstrate stochastic low amplitude pressure fluctuations.

- Triggering occurs upon increasing a bifurcation parameter such as the equivalence ratio, the preheat temperature, the hydrogen content etc.

Quiescence

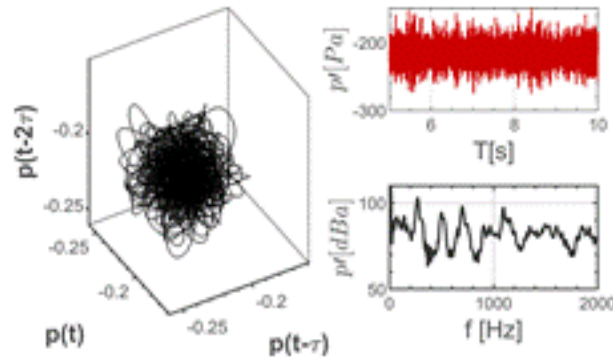


Intermittency

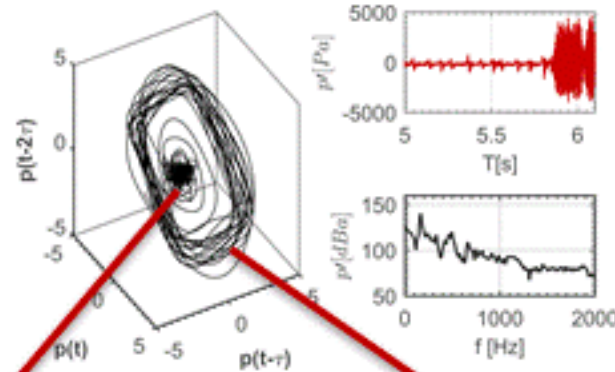


Dynamics: Toroidal transition between limit cycle and fixed point. Emergence of coherent dynamics amidst a quiescent background.

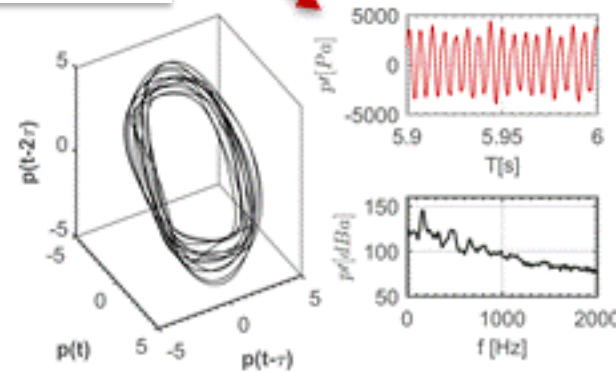
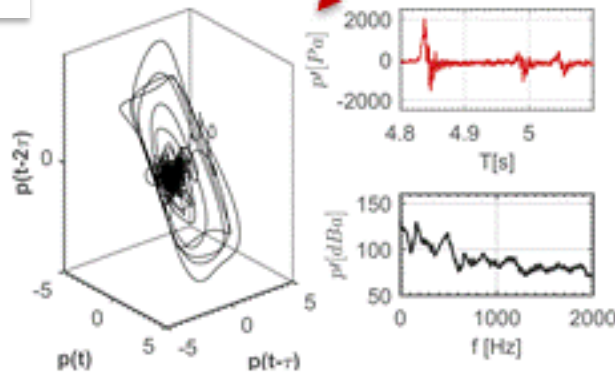
Quiescence



Intermittency

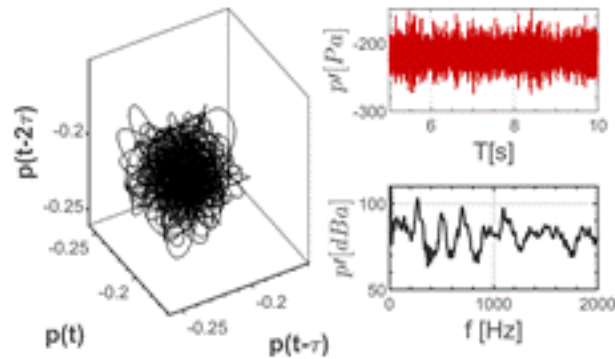


Dynamics: Fixed point and toroidal transition

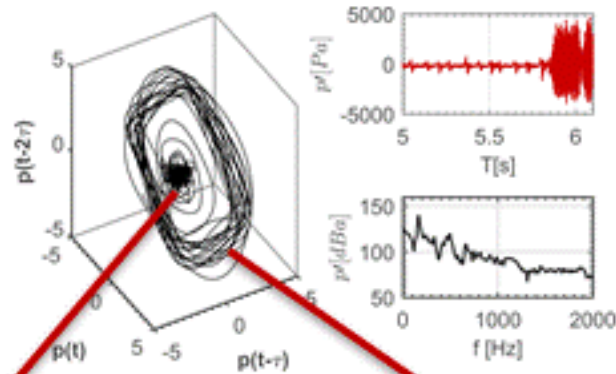


Dynamics: Limit cycle

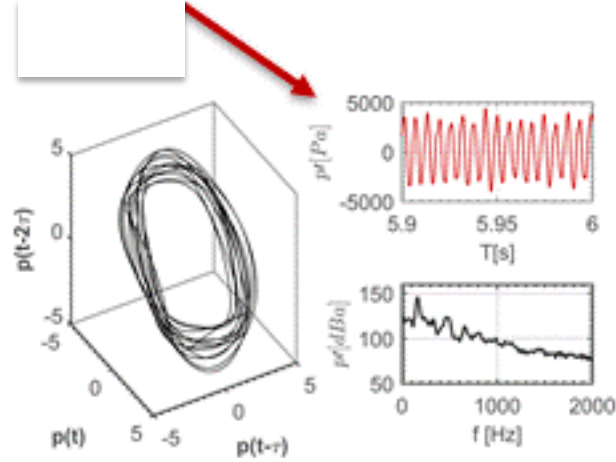
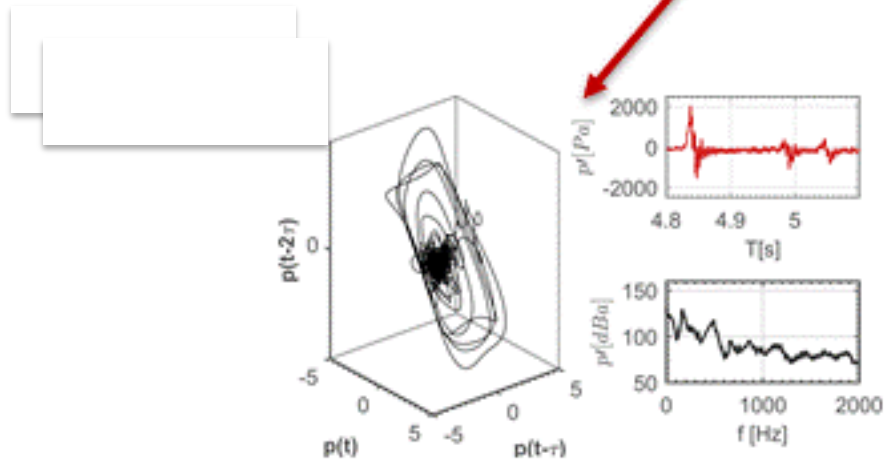
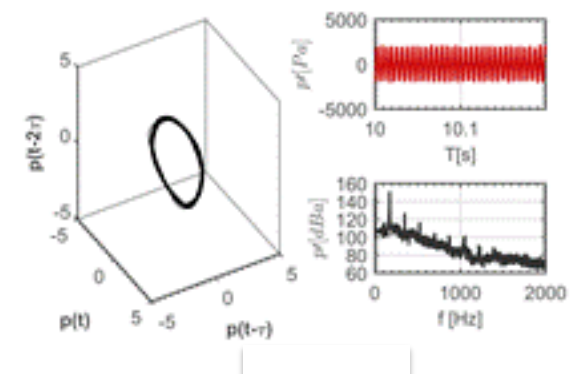
Quiescence



Intermittency



Limit Cycle

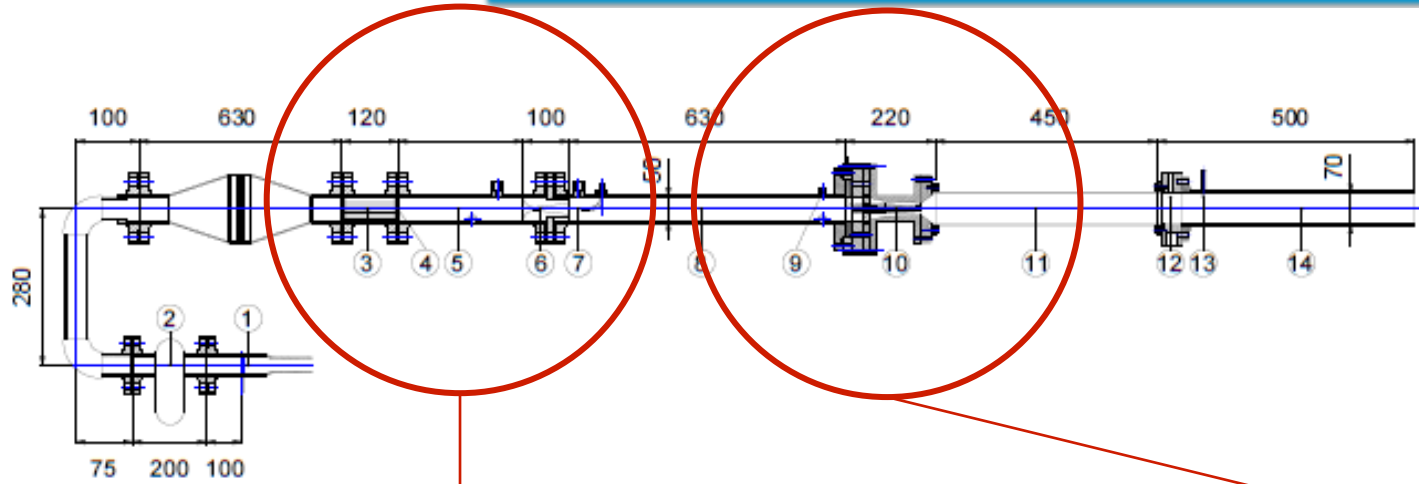


Dynamics:
Consistent attraction
to limit cycle.

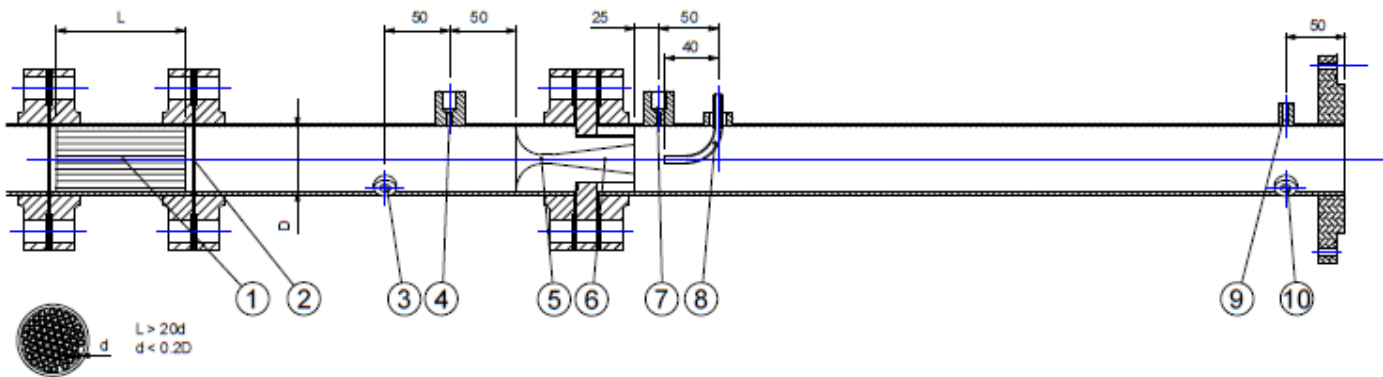
- Increase understanding of physical mechanisms causing the triggering of thermoacoustic instabilities.
- Increase understanding of physical mechanism causing the perpetuation of combustion instabilities.
- Understand how fuel consistency and chemistry affect these mechanisms.

Experimental Configuration

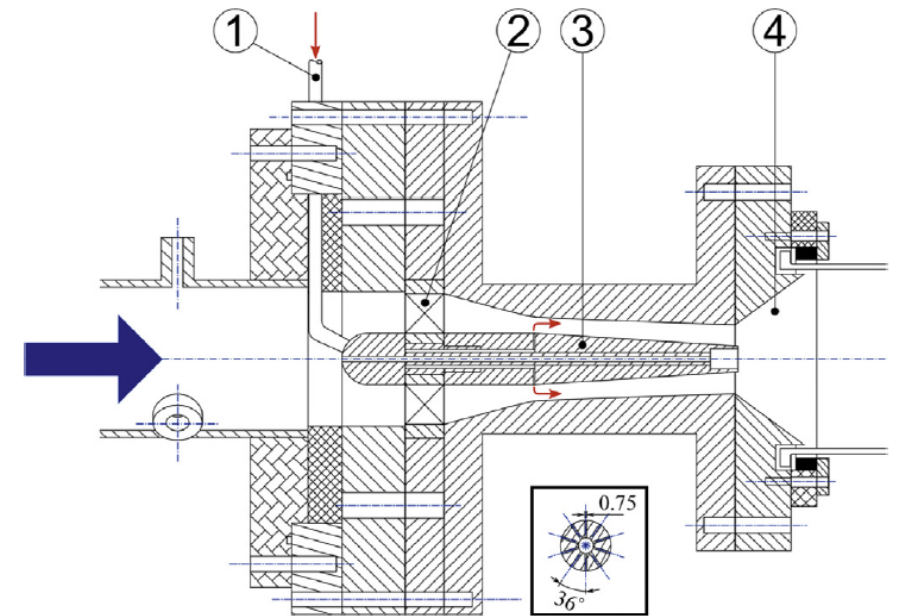
Boundary Conditions



Venturi Nozzle:
Chocked Air Flow

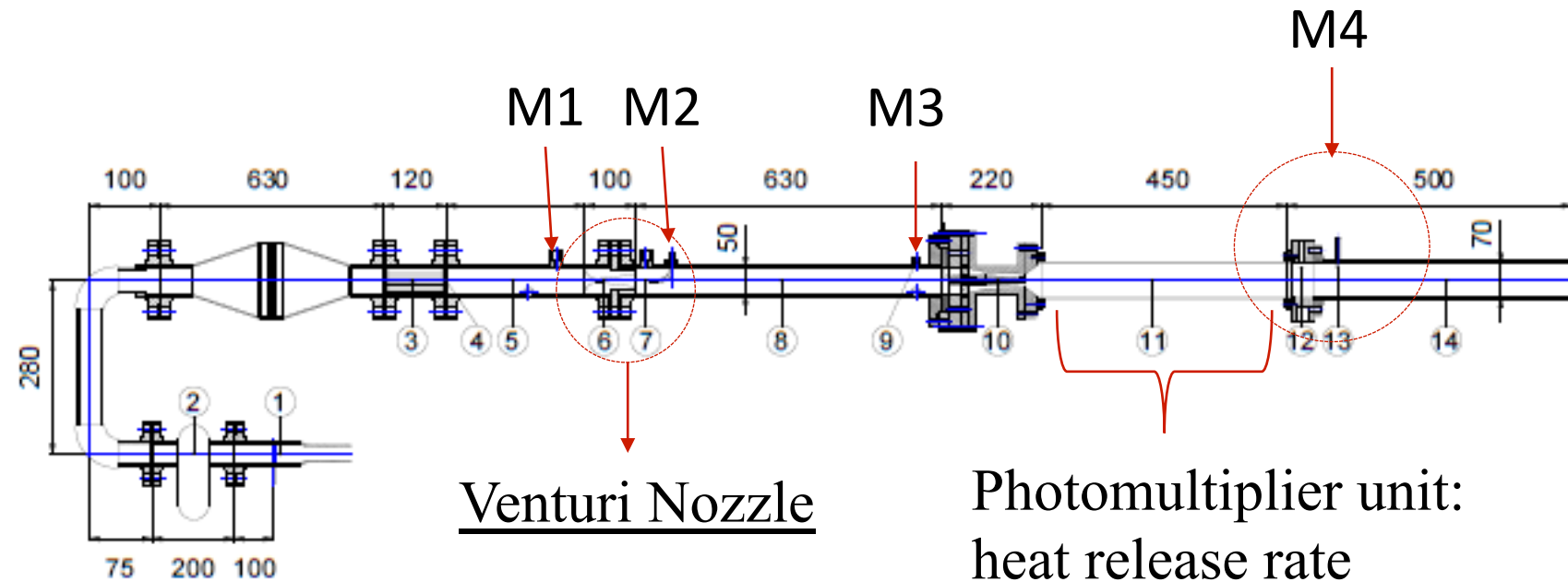


Burner: Chocked Fuel
Injection



Experimental Configuration

Measurement of fundamental quantities



Venturi Nozzle

Photomultiplier unit:
heat release rate
(CH^* , C_2^* , OH^*)

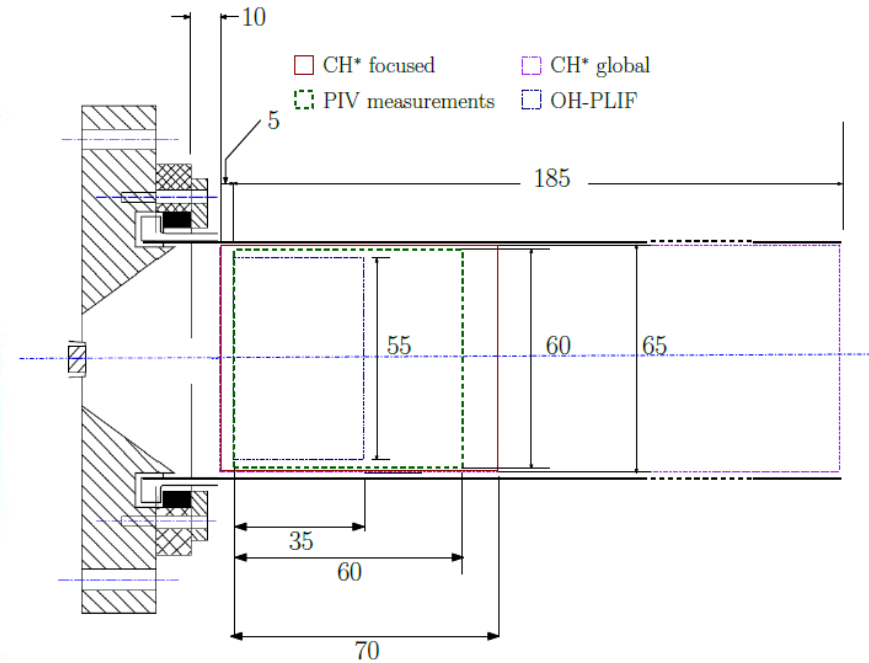
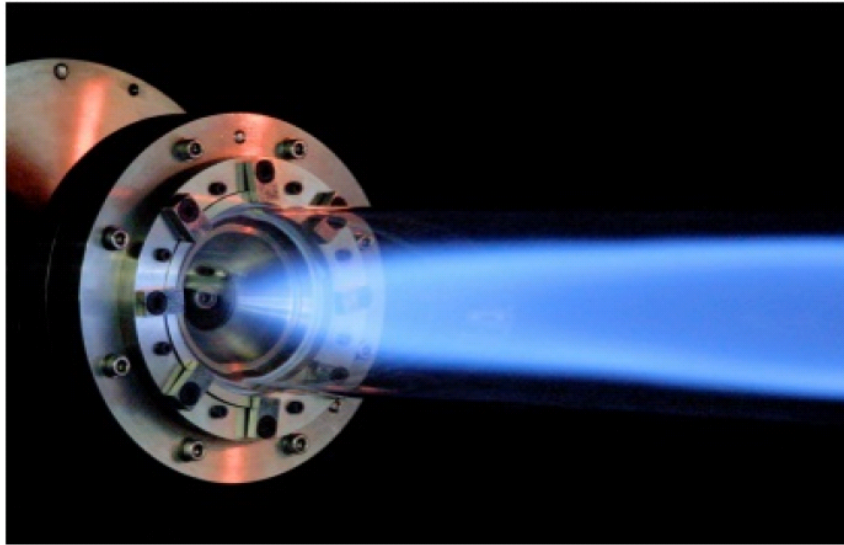
M1, M2: Monitor pressure drop across Venturi nozzle.

M2, M3: Acoustic wave amplitude inside duct (2-mic method)

M4: Standing wave along combustor

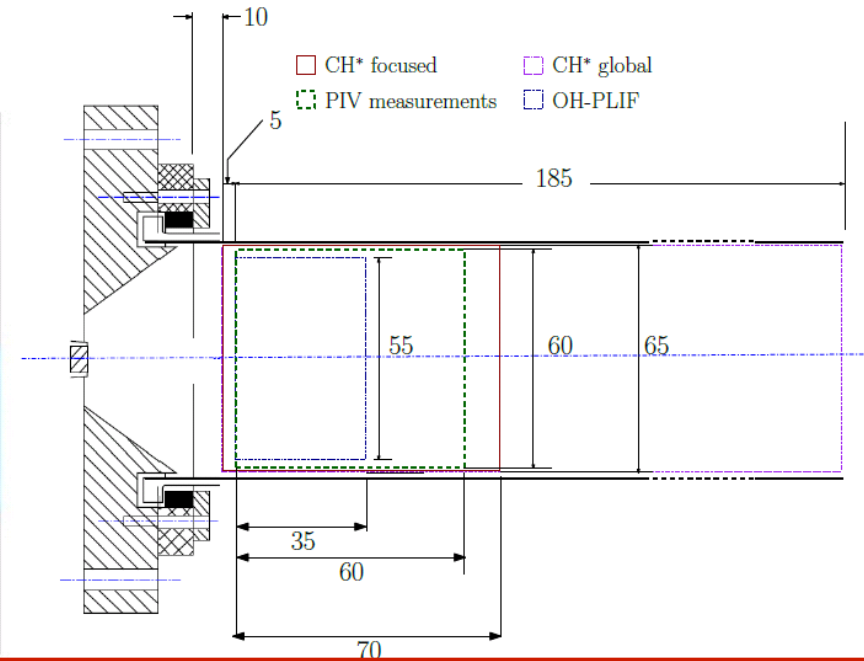
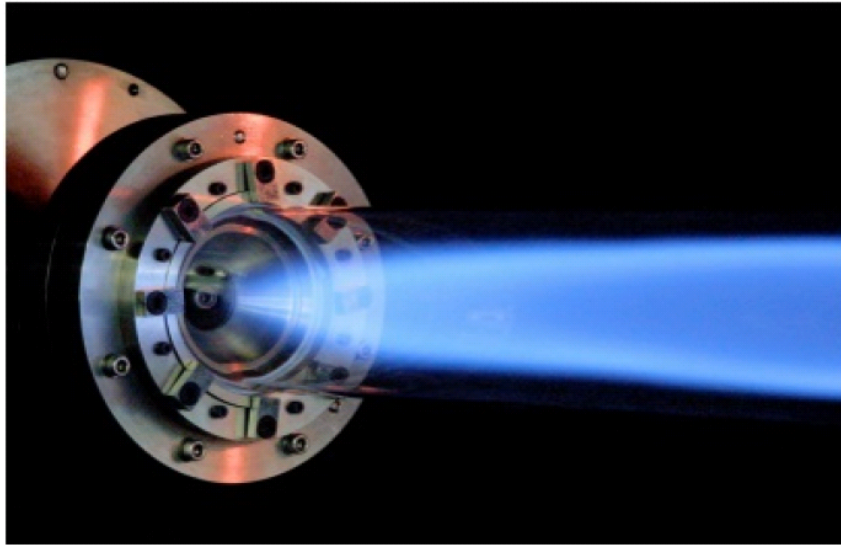
M5 (not shown): Pressure in fuel supply line

Experimental Configuration Swirler and Optically Accessible Combustion Window



Measurement techniques: High speed CH* imaging (3000 Hz), High speed PIV (3000 Hz), OH-LIF (phase conditioned with acoustics), dynamic pressure, PMT integral heat release rate

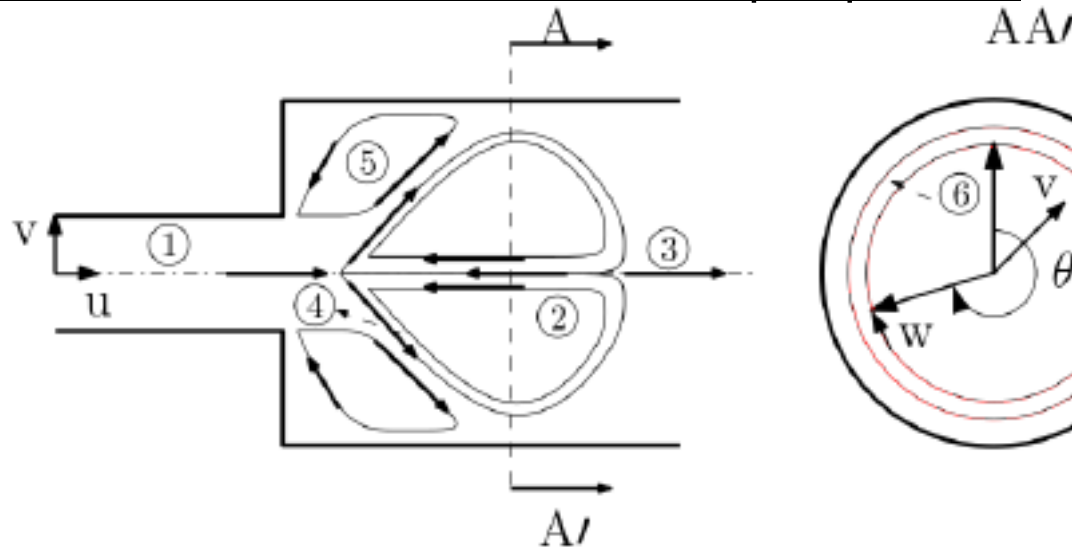
Experimental Configuration Swirler and Optically Accessible Combustion Window



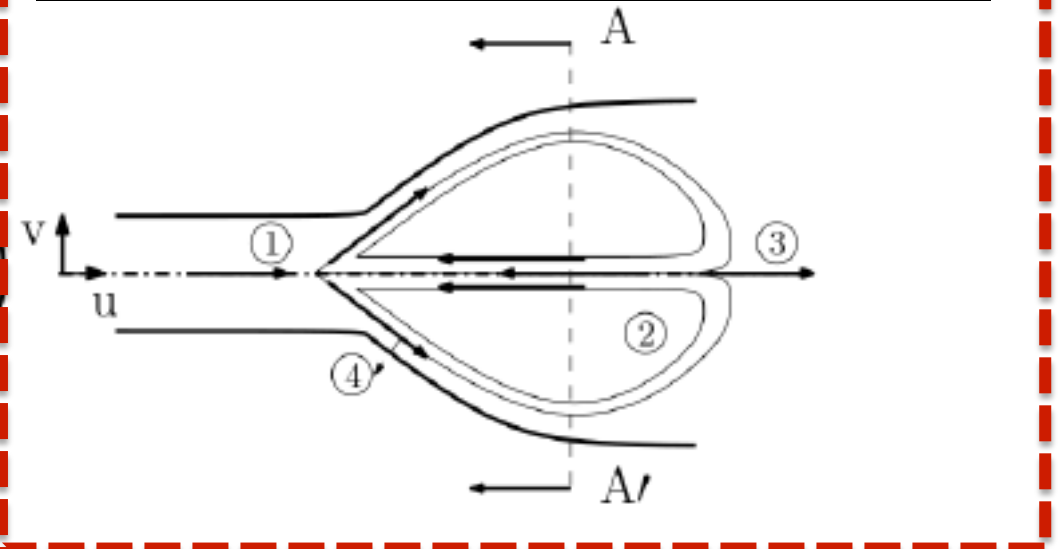
- Geometry remarkable characteristics:
 1. Highly confined nature of the combustor.
 2. The flame is susceptible to touching the combustor walls.
 3. Diffuser prevents the formation of outer recirculation zones.



Flow field structure with sudden-step expansion



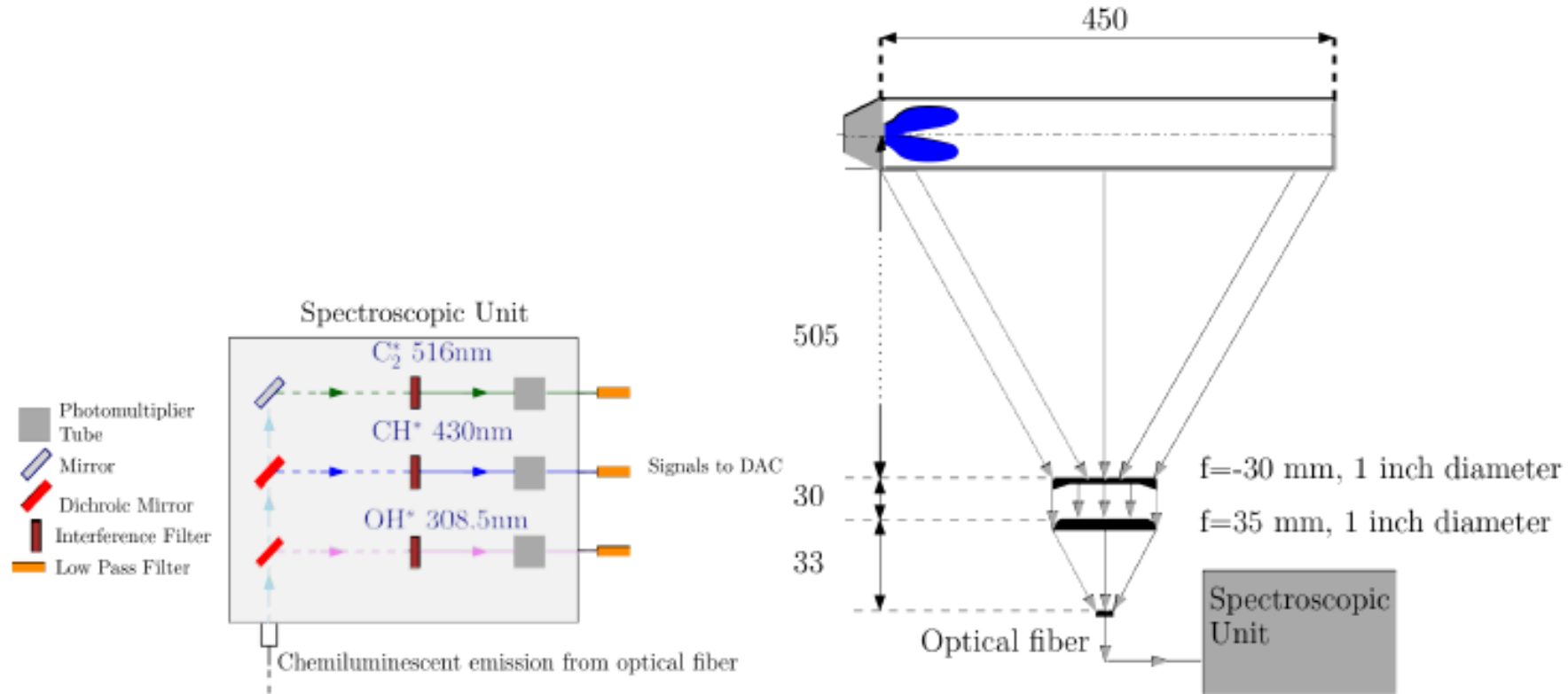
Flow field structure with diffuser at the inlet



- 1. Upstream flow, 2. Inner Recirculation Zone, 3. Downstream flow, 4. Shear Layers, 5. Outer Recirculation Zone.

Experimental Configuration

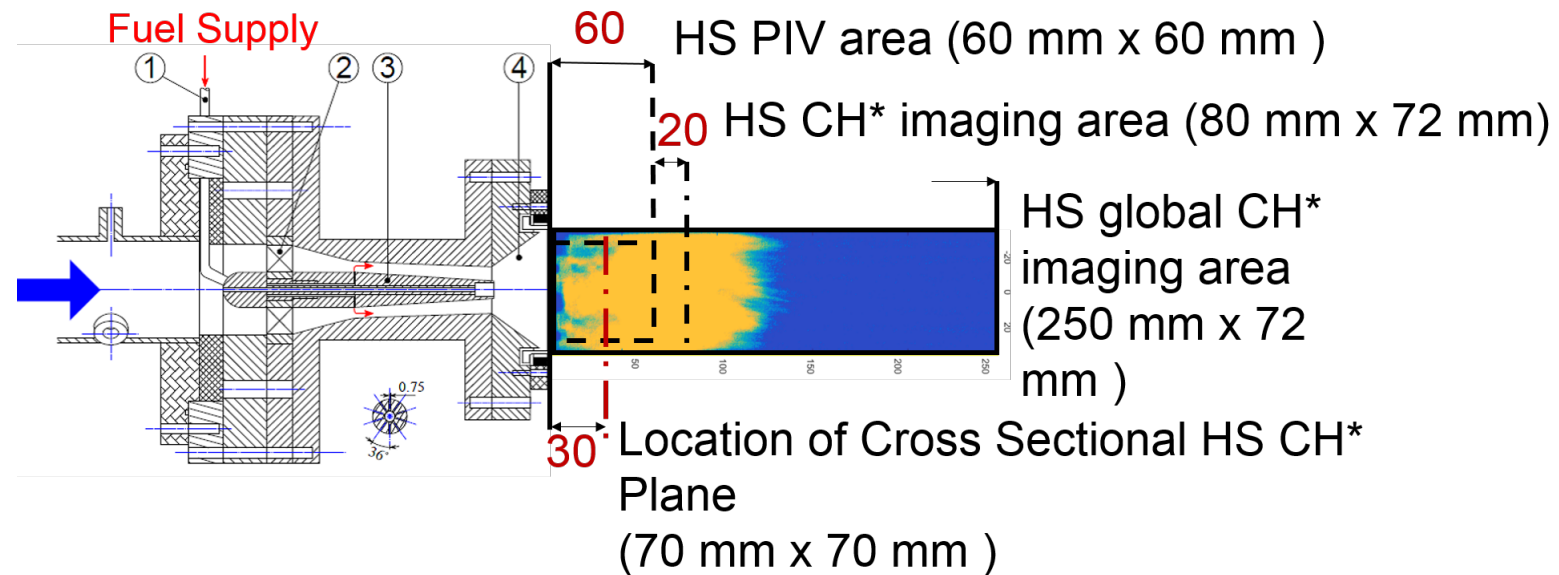
Photomultiplier Tube (PMT) for Chemiluminescent Intensity: Proxy of Global Heat Release



- The integral heat release rate is monitored by the chemiluminescent intensity of species OH^* , CH^* , C_2^*

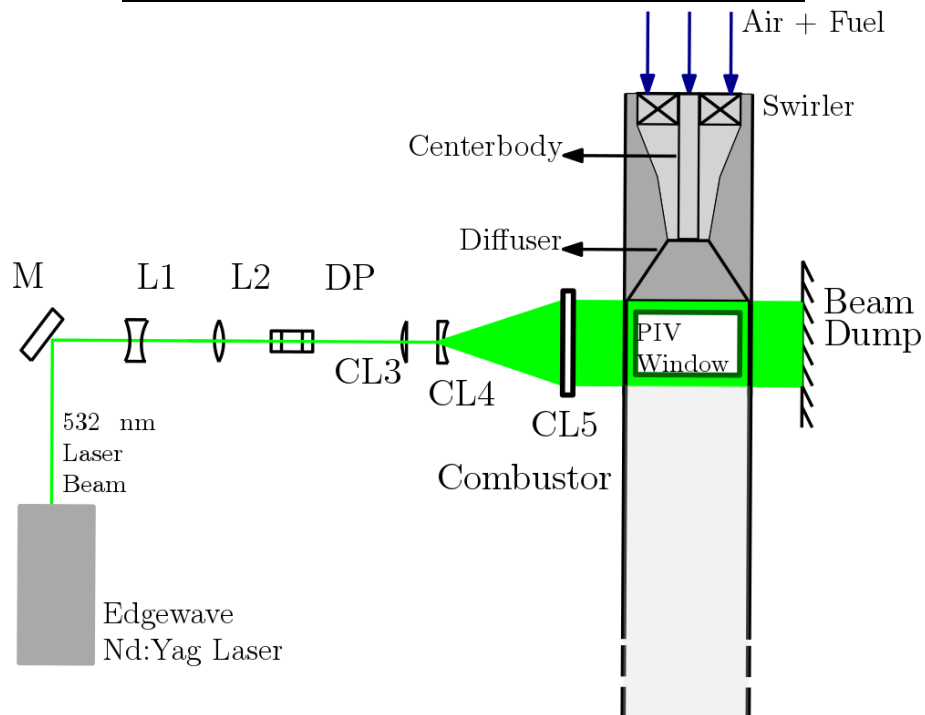
Experimental Configuration

High speed imaging of Chemiluminescent Intensity: Proxy of Heat Release distribution



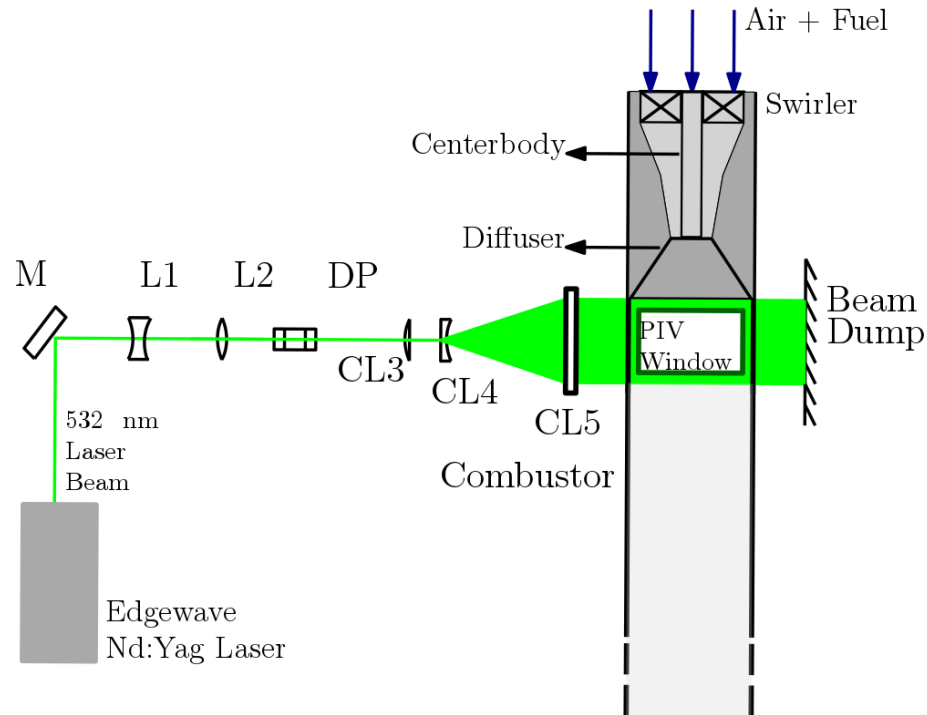
- The spatial distribution of heat release rate is monitored by the High Speed imaging of the chemiluminescent intensity distribution of species OH^* or CH^*

PIV Optical Configuration

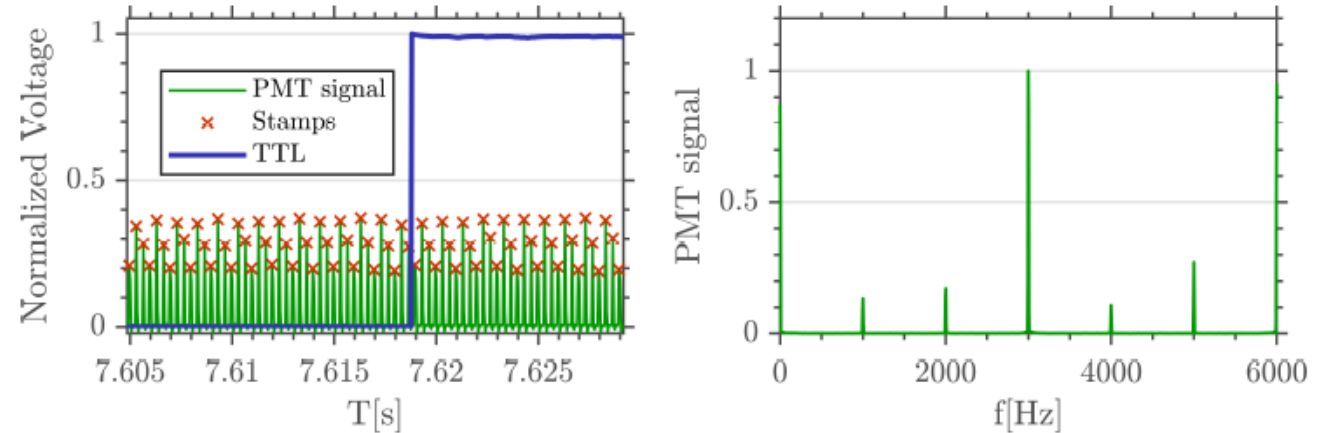


- PIV is an optical diagnostic technique wherein a flow seeded with a heat resistive powder is twice illuminated. The successive images (with a Δt of a few $\sim \mu\text{s}$) yield the velocity field on the illumination plane.
- Challenges:
 - Deposition of particles on combustor walls, limits time window to acquire measurements.
 - Proximity of combustor walls with the flame precipitates deposition of particles.
 - Due to the above, it is very difficult to capture transitions into Subcritical Hopf Bifurcations.

PIV Optical Configuration

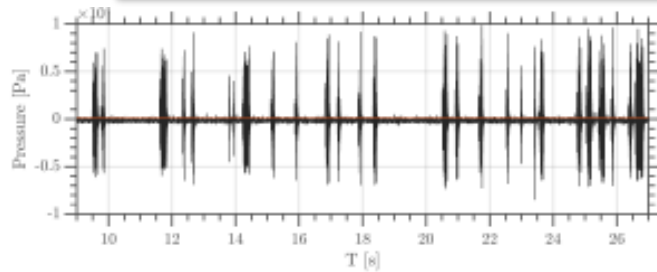


PIV Synchronisation Signal

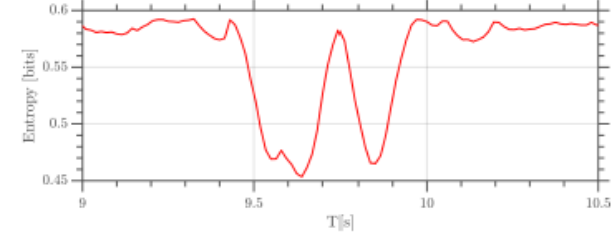
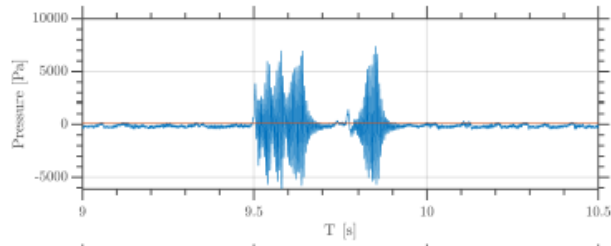
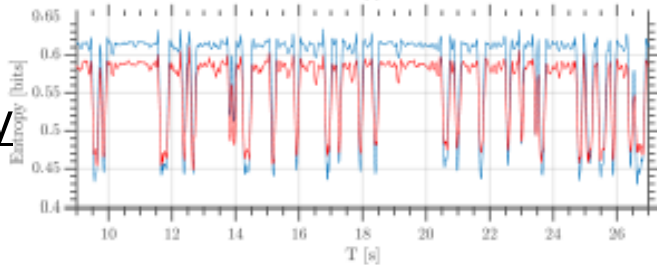


$dt=4\mu s$, 3000 Hz, FOV: 60 mm x 60 mm, Interrogation windows 16 x 16 pixels, 75% overlap, Resolution: 0.23 mm, Nominal uncertainty: 0.06 m/s.

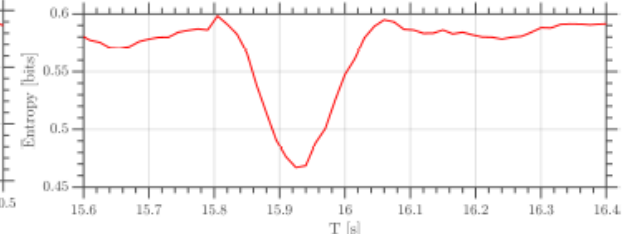
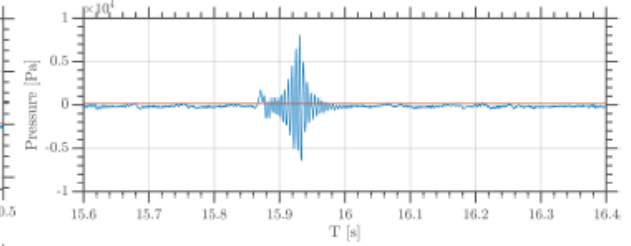
Dynamic Pressure



Permutation Entropy



(a) T=[9 s-10.5 s]



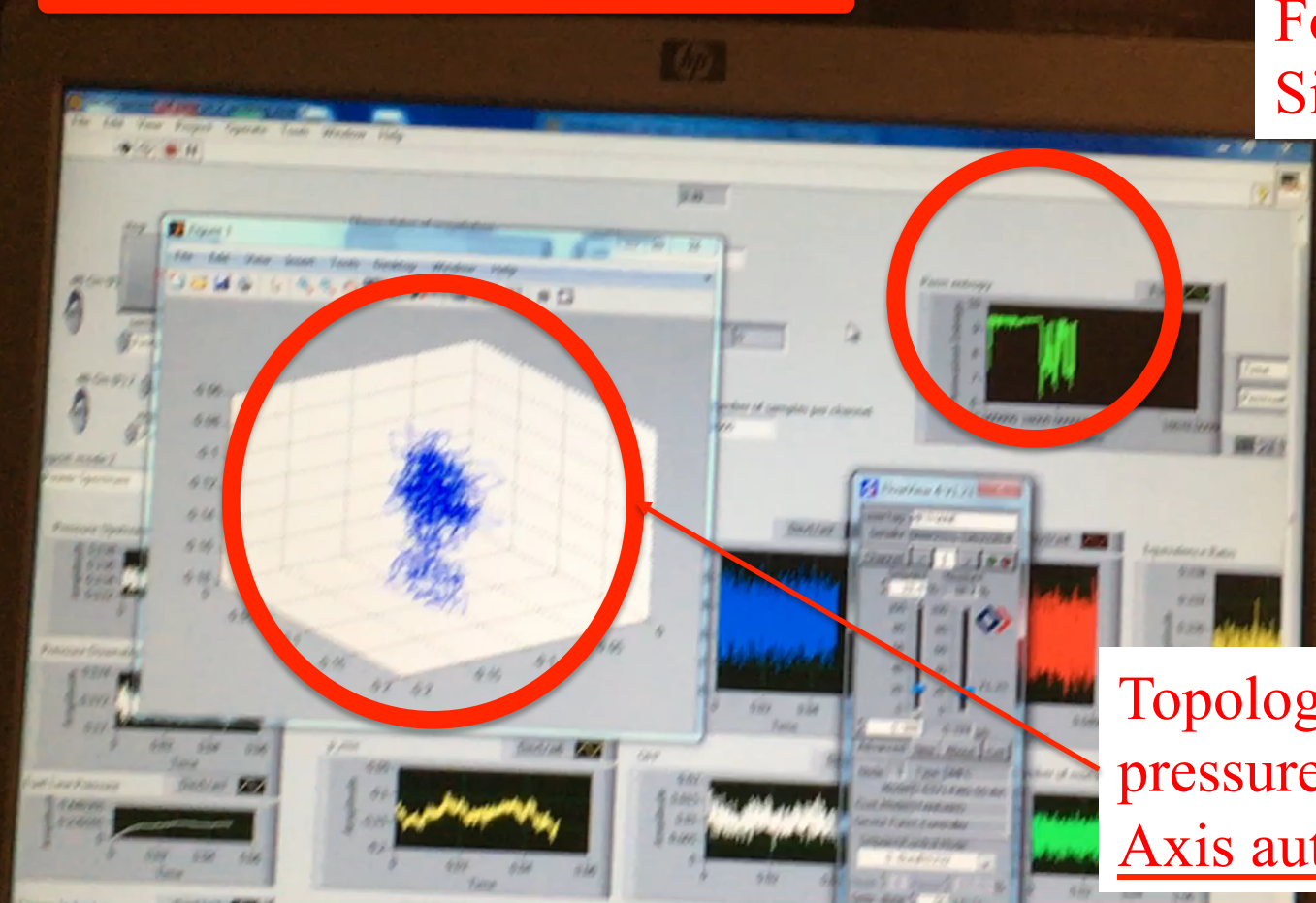
(b) T=[15.6 s-16.4 s]

- Since transition into thermoacoustic instability is accompanied with loss of randomness and emergence of periodicity, a short term prediction algorithm is required to quantify this transition.
- The permutation entropy was implemented online in order to trigger the PIV diagnostics and capture the transition into thermoacoustic instability, thus avoiding ‘seeding’ particle deposition problems during acquisition.
- The permutation entropy is a measure of the complexity of the time series. A higher number of possible permutations corresponds to a stochastic aperiodic state.



Unstable Premixed Flame

Forewarning
Signal

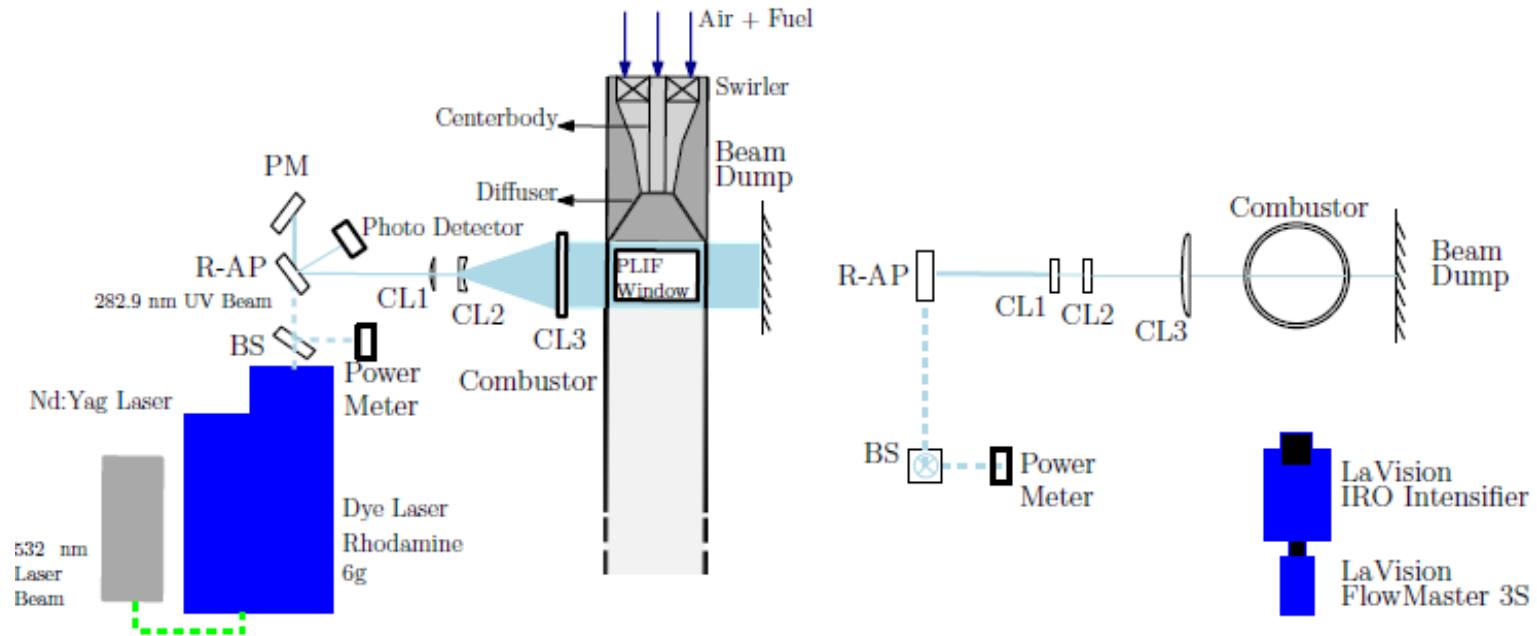


Topology of attraction of dynamic
pressure signal in phase space
Axis auto adjuste scaling

Experimental Configuration

Planar Laser Induced Fluorescence (PLIF) Measurements

PLIF Optical Configuration

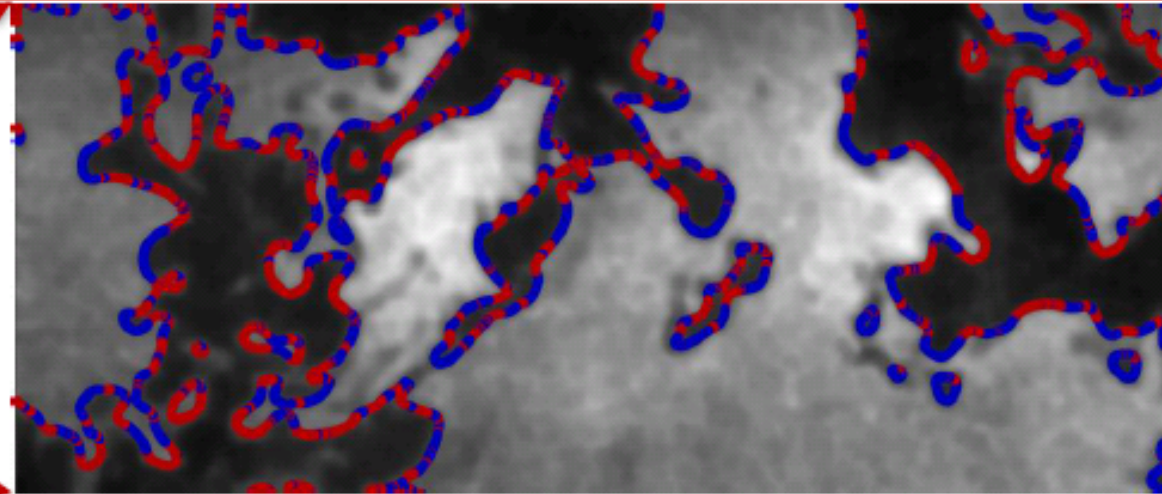
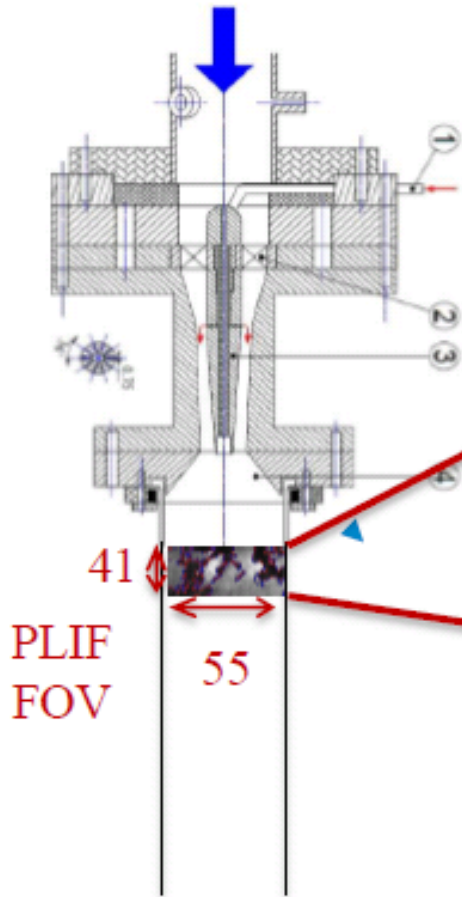


10 Hz, excitation $Q_1(6)$ transition line: $A^2\Sigma-X^2\Pi$ at 282.9 nm, light collected at 308 nm and 314 nm, dye laser output: 18mJ per pulse, field of view 35 mm x 35 mm, resolution of 5 line pairs / mm (curvature resolution)

Flame front curvature analysis

Flame front detection algorithm

Method: [Bayley et al., 2012] Bayley, A. E., Hardalupas, Y., & Taylor, A. M. (2012). Local curvature measurements of a lean, partially premixed swirl-stabilised flame. Experiments in Fluids, 52(4), 963–983.



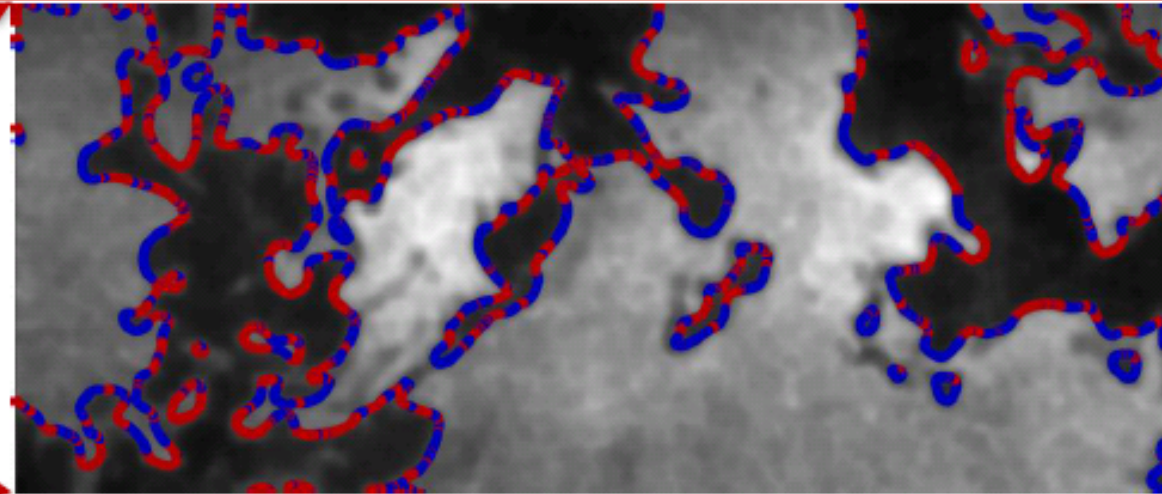
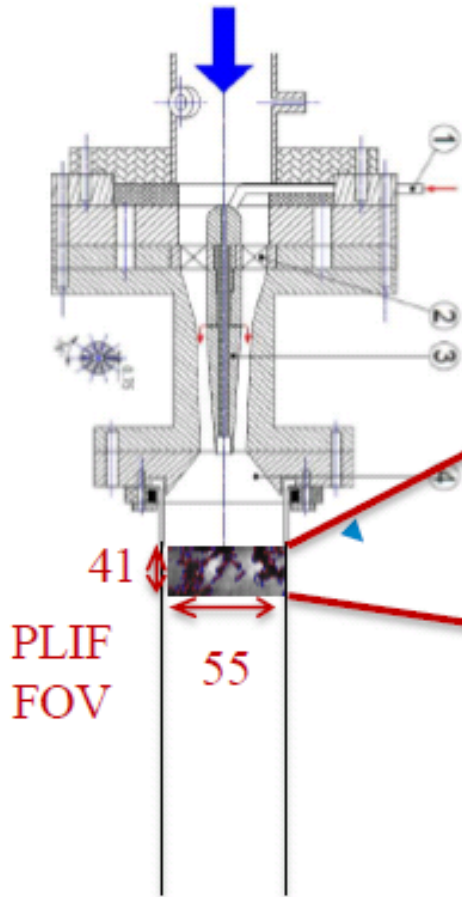
— Burned (Unburned
Negative curvature

Burned) Unburned +
Positive curvature

Flame front curvature analysis

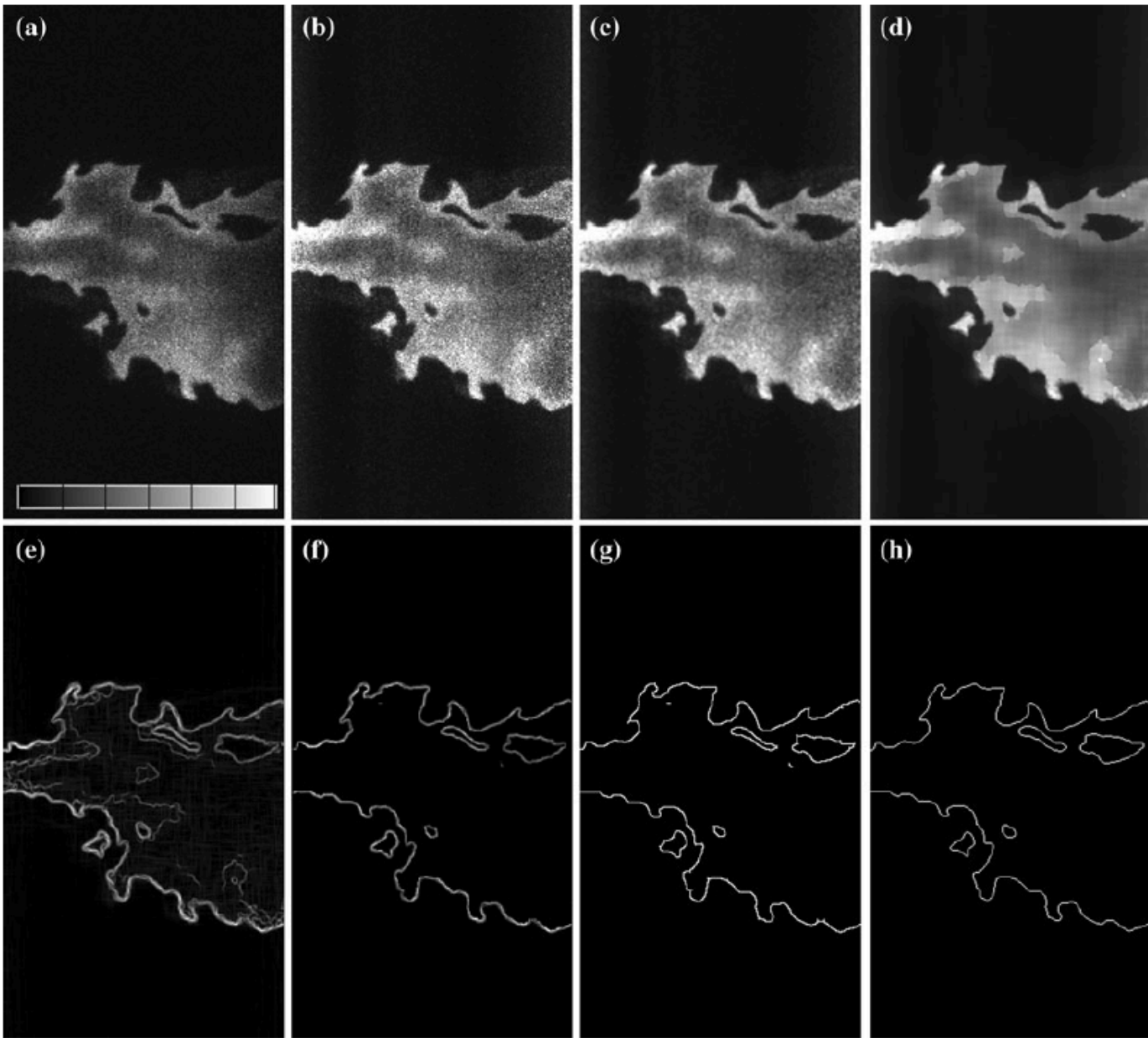
Flame front detection algorithm

Method: [Bayley et al., 2012] Bayley, A. E., Hardalupas, Y., & Taylor, A. M. (2012). Local curvature measurements of a lean, partially premixed swirl-stabilised flame. Experiments in Fluids, 52(4), 963–983.

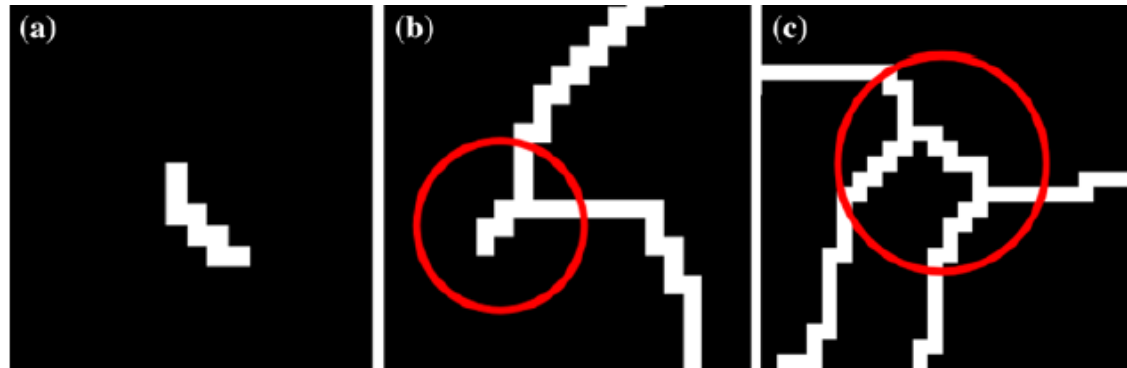


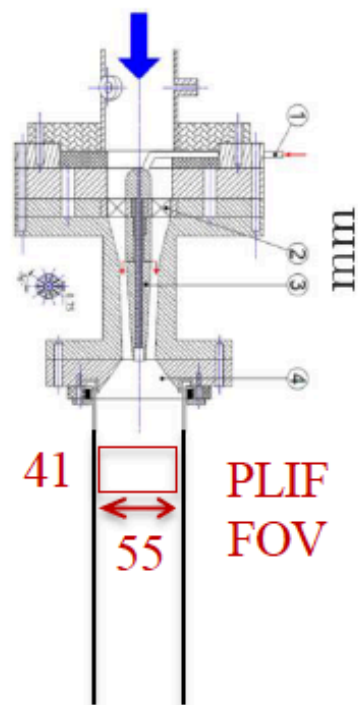
— Burned (Unburned
Negative curvature

Burned) Unburned +
Positive curvature

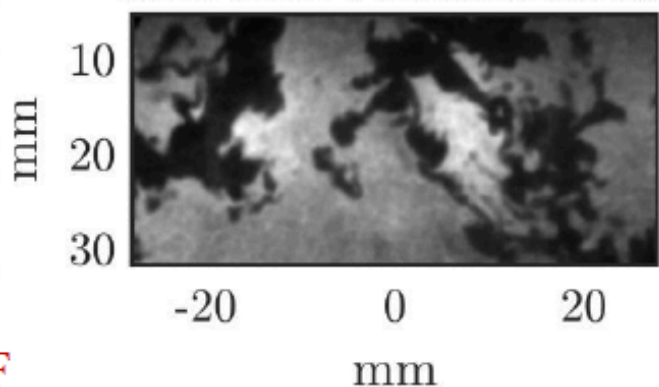


Method avoids the erroneous cases as in the following examples and ensures that the flame curvature is measured accurately.

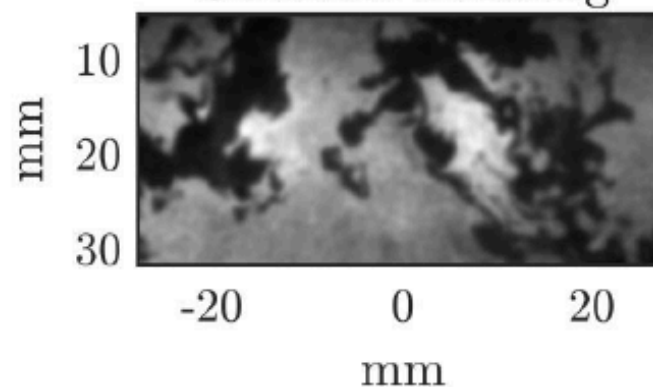




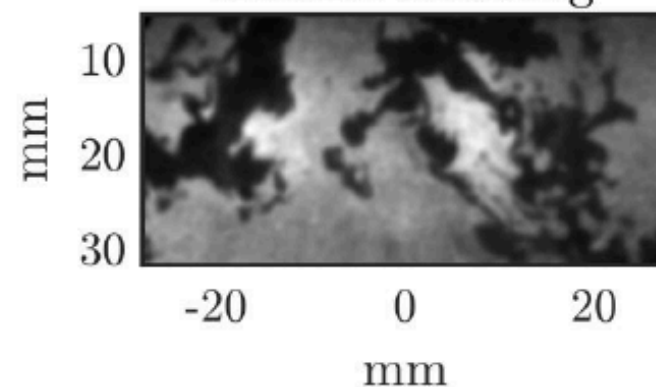
Min-Max Normalization



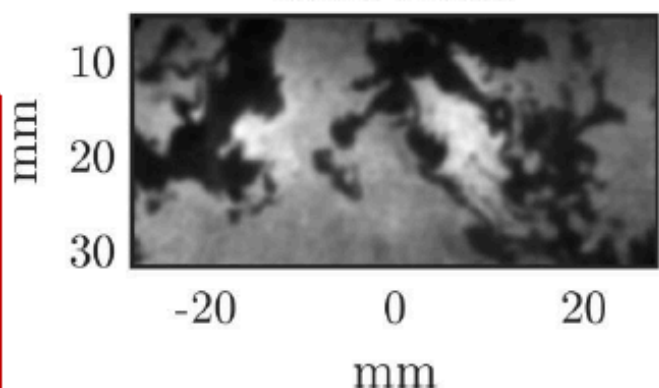
Gaussian Filtering



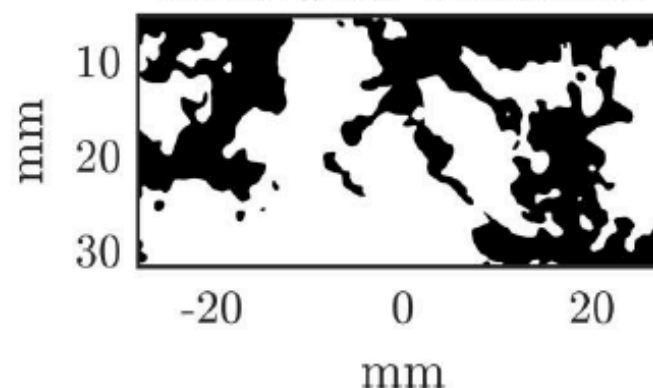
Median Filtering



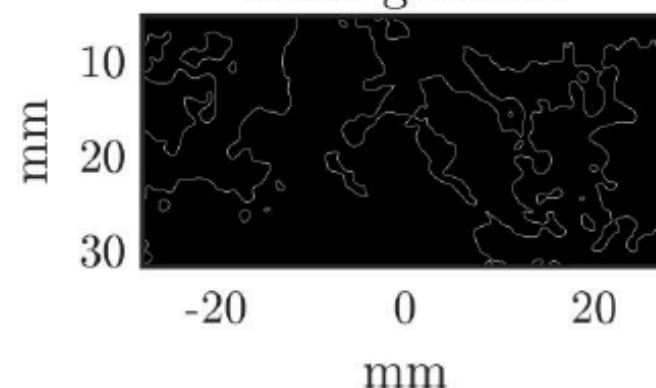
NLD Filter



Multi-level Threshold



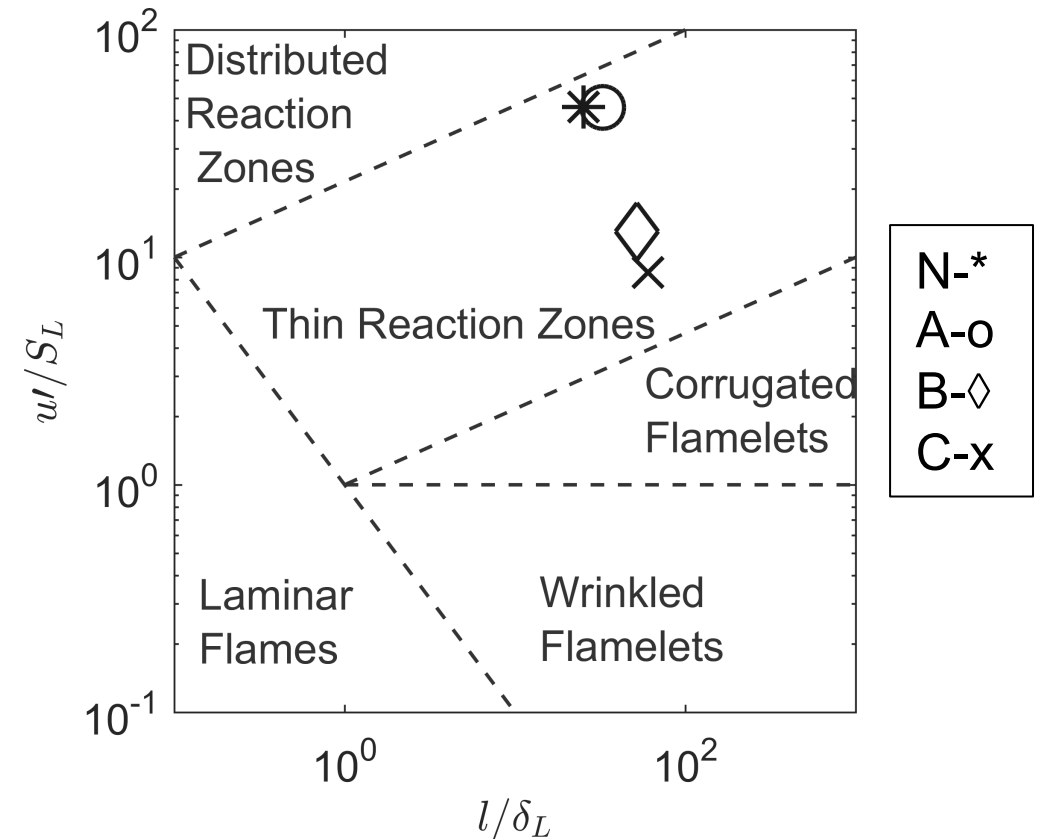
Sobel gradient



Resolution:
1376 x 1040
FOV: 55.135 mm x
41.659 mm
Resolvable curvature:
5 line pairs / mm

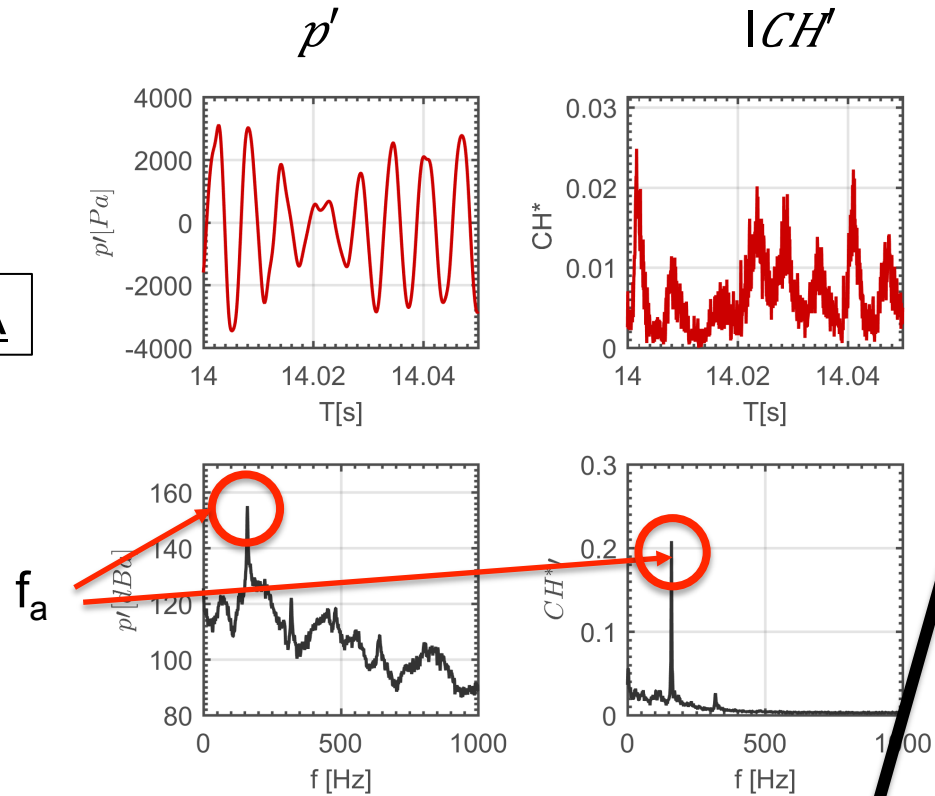
Period – 2 Limit Cycle

Case ID	ϕ	Dynamic State	K_{ext} [1/s]
N	0.50	Intermittent	85
A	0.55	Period-1	236
B	0.60	Period-2	608
C	0.65	Period-2	1138

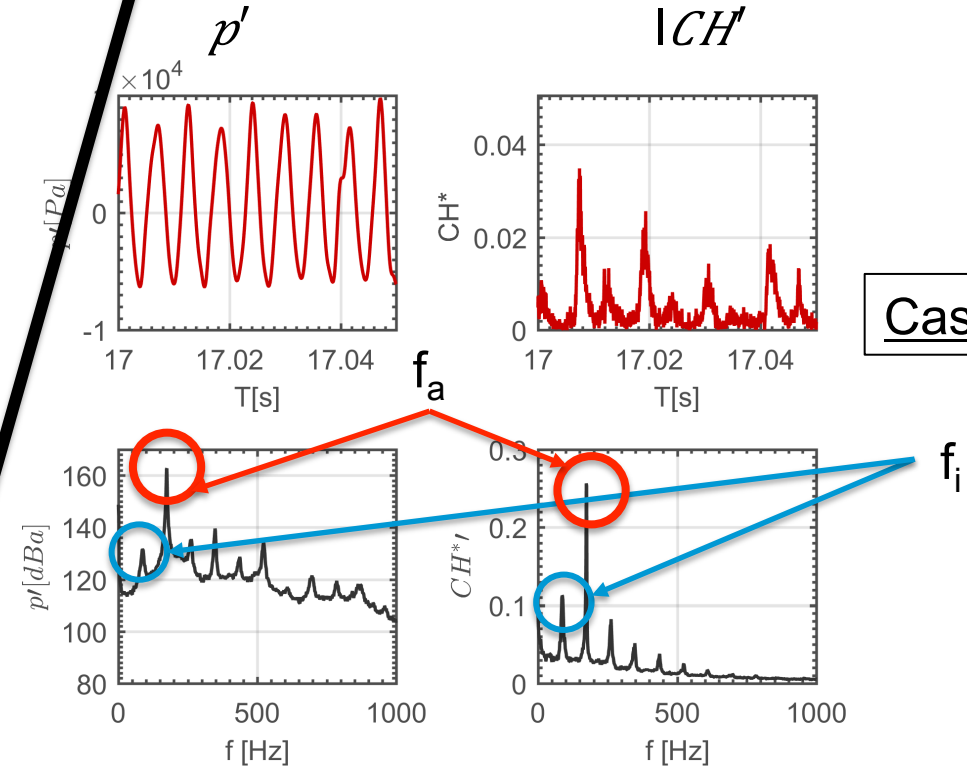


Manifestation of Period Doubling Bifurcation

Case A



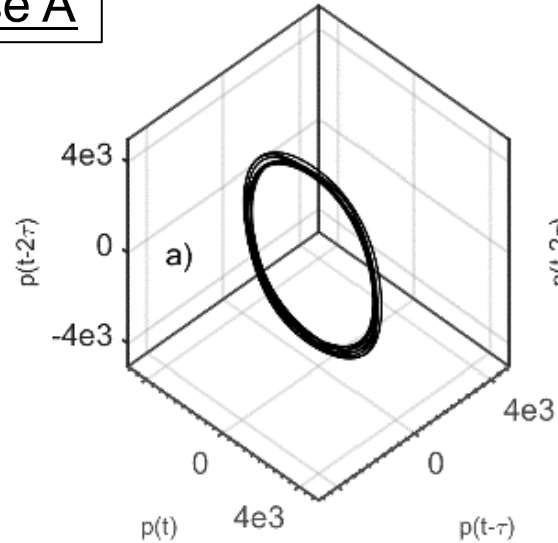
Case B



- On increasing φ under constant Re , the dynamics are attracted from a Period-1 limit cycle to a Period-2 limit cycle.

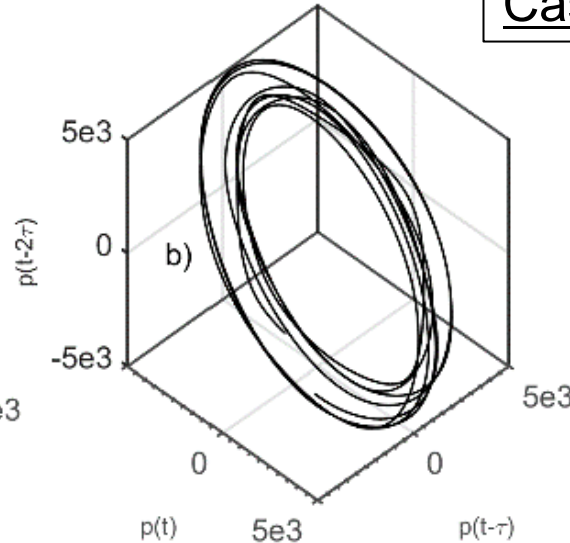
Manifestation of Period Doubling Bifurcation

Case A



Period 1 Limit Cycle

Case B



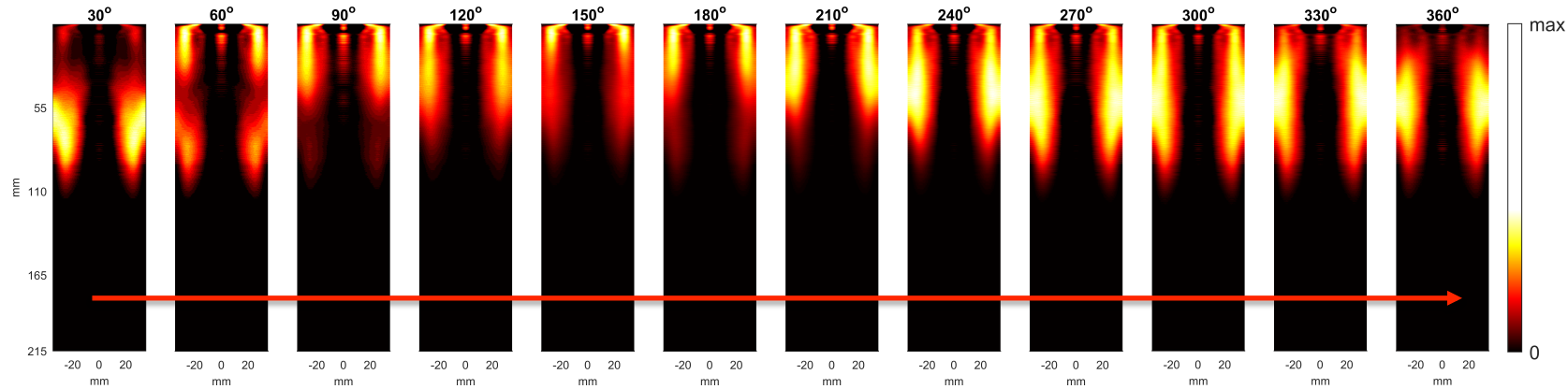
Period 2 Limit Cycle

- On increasing ϕ under constant Re , the dynamics are attracted from a Period-1 limit cycle to a Period-2 limit cycle.

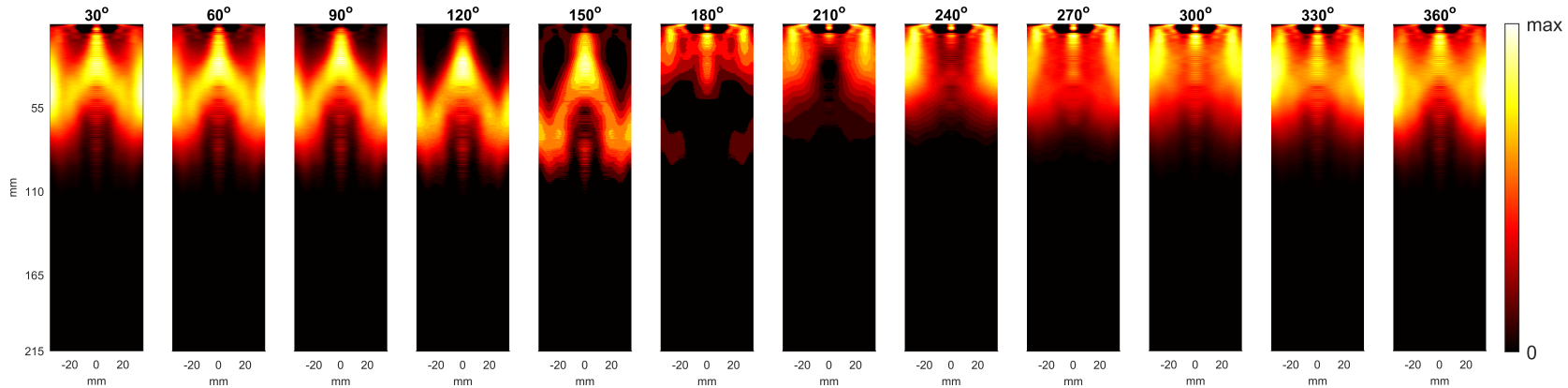
Manifestation of Period Doubling Bifurcation Flame shape effects

Case A

Phase averaged
structure

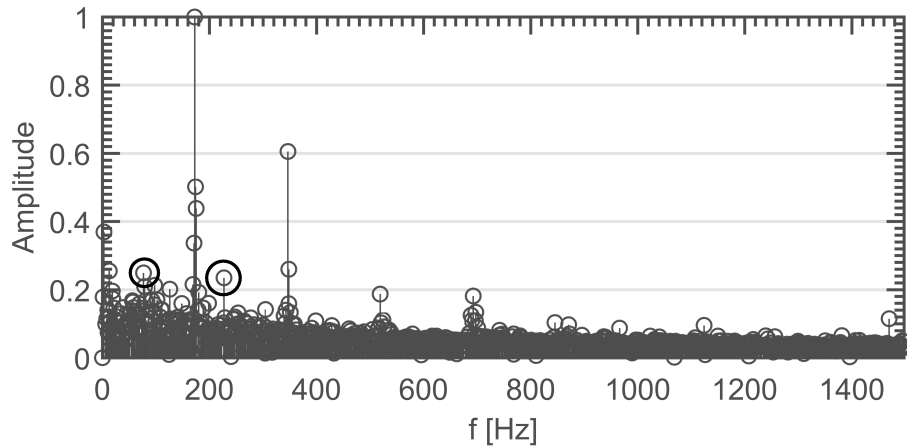


Case B

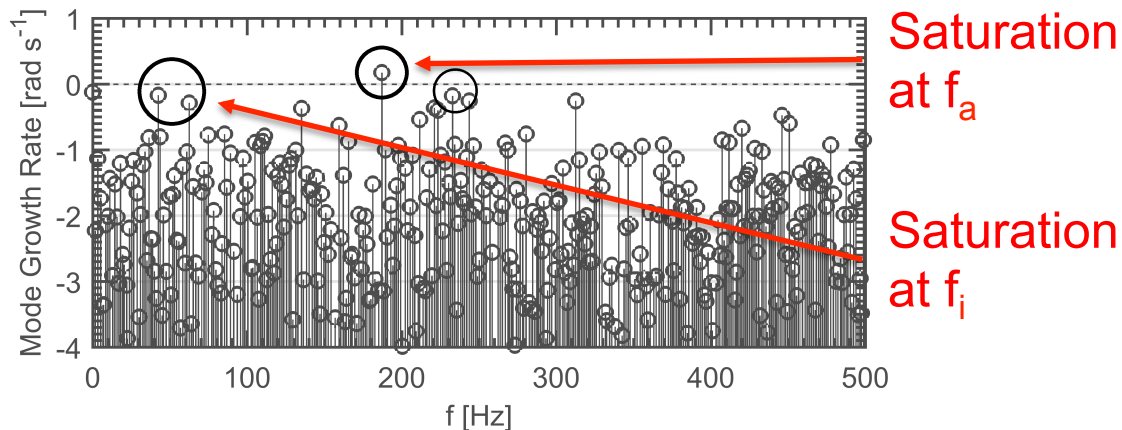


- The period 1 and period 2 flames assumes a V and M shape respectively.
- Phase averaged flame shape with respect to the fundamental frequency of instabilities.

DMD Modes Amplitude



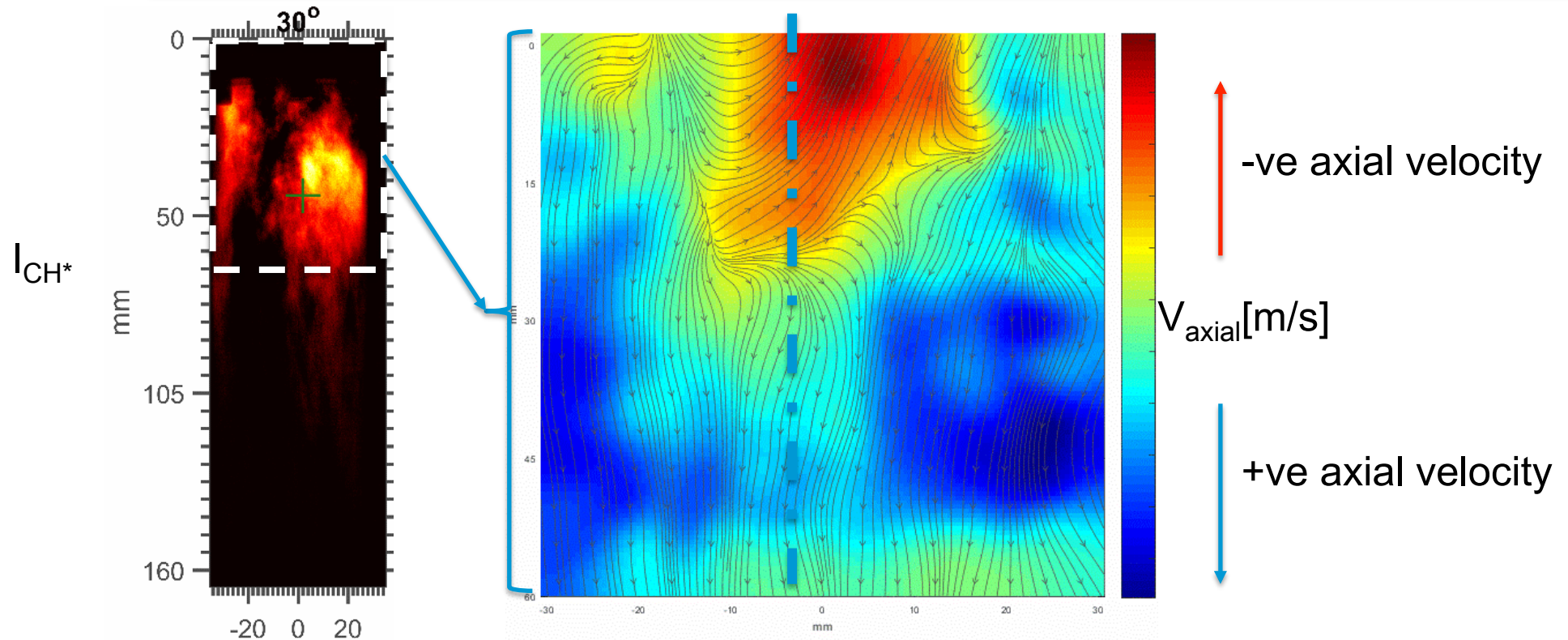
DMD Modes Growth Rate



- Dynamic Mode Decomposition calculates temporally orthogonal modes to associate phenomena observed in n temporally equidistant snapshots $\{v_1, v_2, \dots, v_n\}$ to a single specific frequency and growth rate.
- Reconstruction in the temporal domain is achieved by selecting the frequencies and reconstructing.

Manifestation of Period Doubling Bifurcation

Nature of the subharmonic frequency



- DMD assists in extracting the flame structure at the subharmonic frequency of interest.
- Under the effect of PVC: azimuthal convection of high heat release disturbance, wherein intensity is skewed towards the right half of the cylinder.

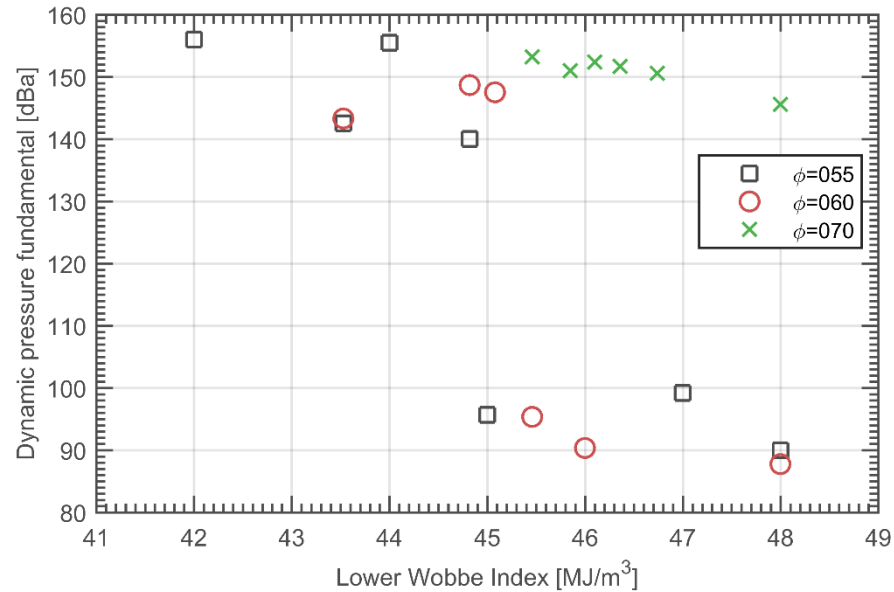
Interpretation of what triggers the Combustion instabilities

Research aim 1: Interpretation of what triggers the Combustion instabilities

- This section interprets the triggering mechanisms of combustion instabilities.
- The combustor is driven through Quiescence-Intermittency-Limit Cycle dynamics by enriching methane with hydrogen.
- It will be shown that the hydrogen molar content increases the extinction strain rate (k_{ext}) of the premixture and this characteristic quantity can largely collapse the transitions.
- Link between thermoacoustic dynamics and flame front curvature.

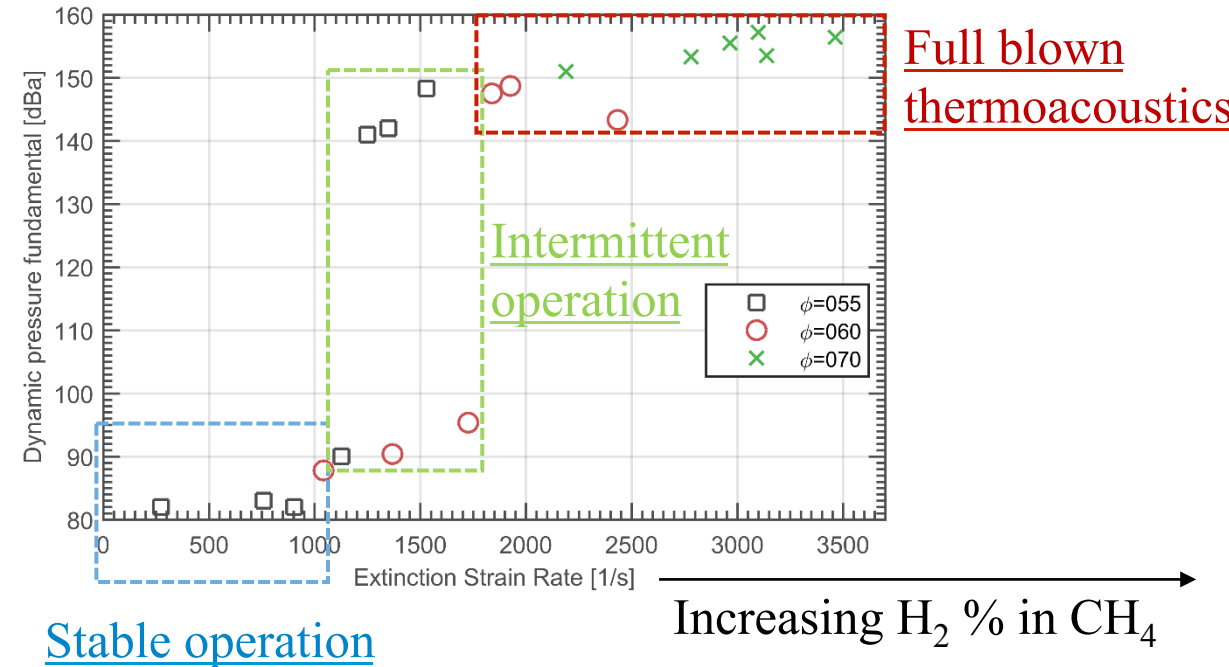
Motivation: Extinction strain rate is a mixture property collapsing dynamic state transitions (H₂ enriched CH₄ blends)

Collapsing dynamics with Wobbe index



Lower Wobbe Index $LWI = LHV / \sqrt{SG}$ [MJ/m³]

Collapsing dynamics with extinction strain rate



Karlis, E., Liu, Y. Hardalupas, Y., & Taylor, A. M. (2020) Extinction strain rate suppression of the precessing vortex core in a swirl stabilised combustor and consequences for thermoacoustic oscillations. Combustion and Flame, 211(3), 229-252.

Karlis, E., Liu, Y. Hardalupas, Y., & Taylor, A. M. (2019d) H₂ enrichment of CH₄ blends in lean premixed gas turbine combustion: An experimental study on effects on flame shape and thermoacoustic oscillations dynamics. Fuel, 254, 115524

Description of dynamic states: Focus on the intermittent regimes

Global operational quantities:

Bulk Reynolds number $Re = 19000$

Equivalence ratio $\phi = 0.55$

Mixture ID	Methane molar percentage $\chi:\text{CH}_4$	Hydrogen molar percentage $\chi:\text{H}_2$	Extinction Strain Rate [1/s]	Dynamic State	Le_χ
Case A	1.000	0.000	273	Susceptible to blow off	0.998
Case B	0.900	0.100	652	Quiescent, lifted	0.927
Case C	0.800	0.200	759	Quiescent, lifted	0.856
Case D	0.700	0.300	1127	Intermittent	0.784
Case E	0.650	0.350	1250	Intermittent	0.748
Case F	0.625	0.375	1350	Intermittent	0.731
Case G	0.600	0.400	1540	Limit Cycle	0.713

Presented sample dynamics acquired from Case D

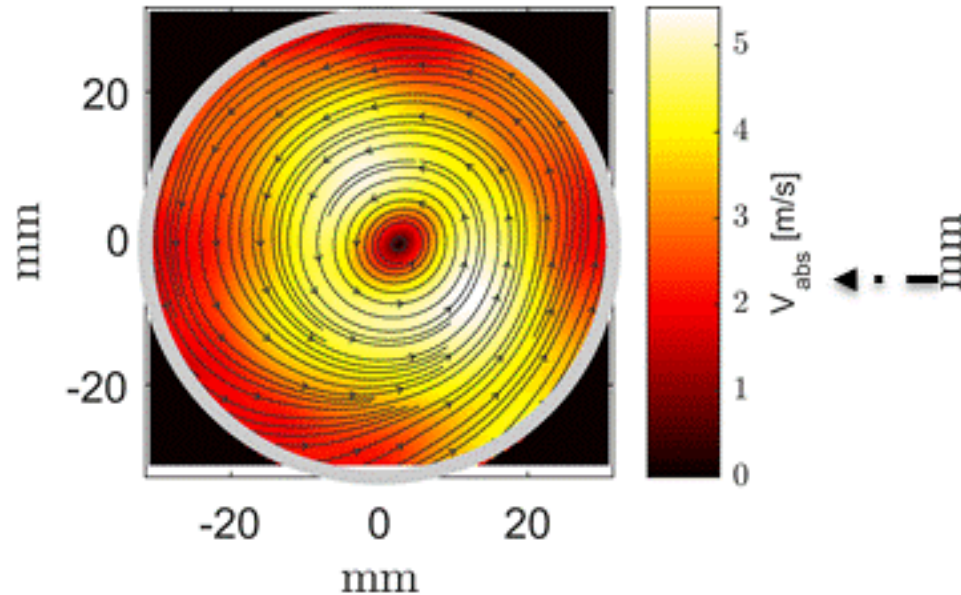
Limit cycle dynamics examined based on case G

Isothermal flowfield and quiescent flame structure

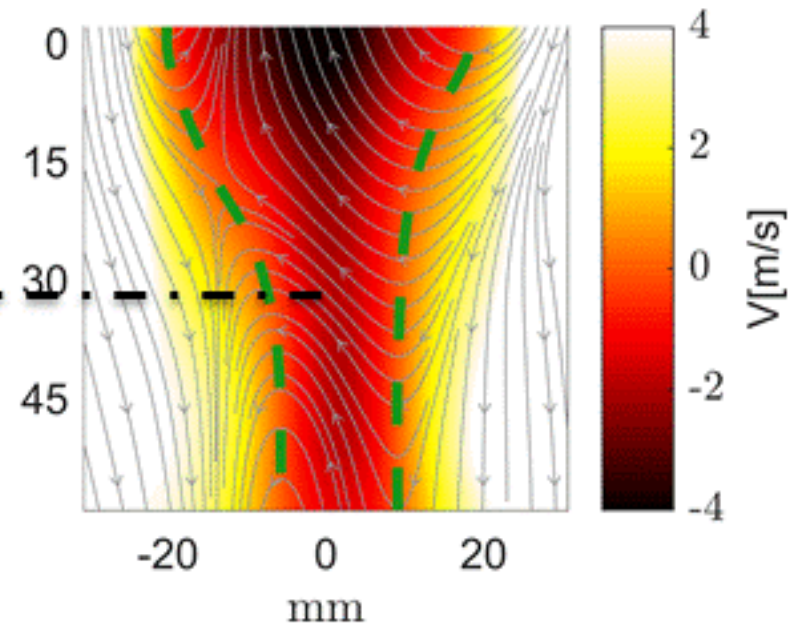
Experimental Configuration

Isothermal-Particle Image Velocimetry (PIV) Measurements

Azimuthal Radial FOV

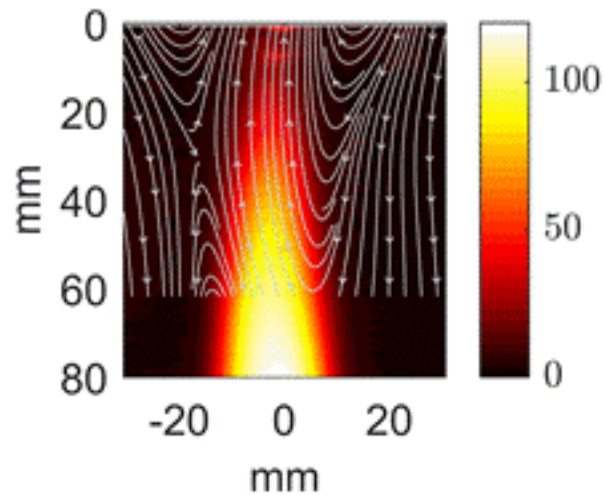


Axial radial FOV

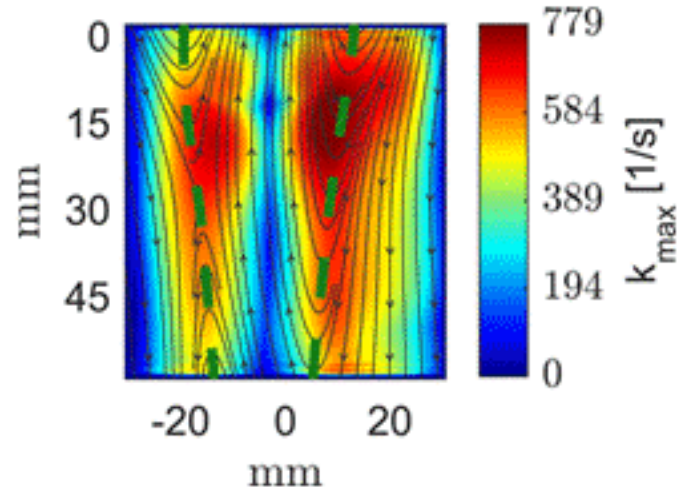


Axial-radial plane: isothermal flow features a recirculation zone with no downstream stagnation point, extending through all section of the PIV FOV

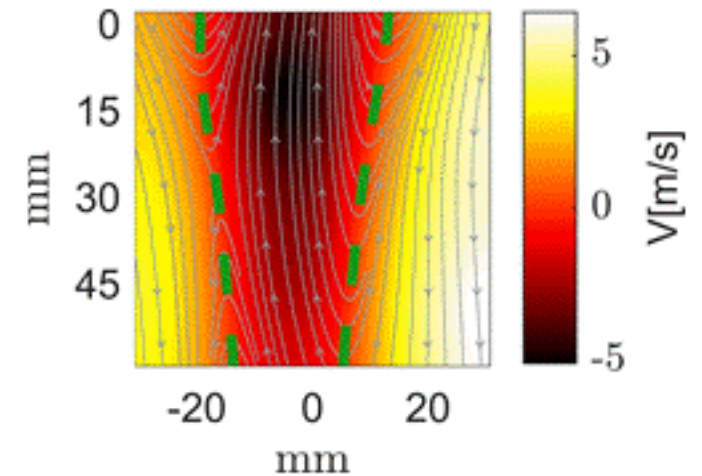
Quiescent flame



Axial-radial strain rate

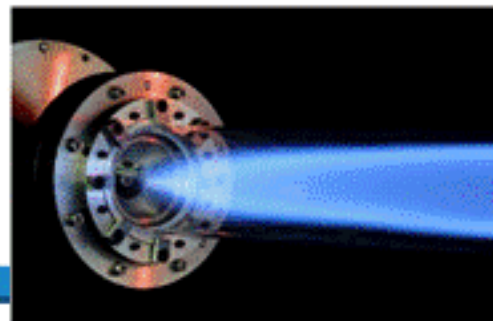


Axial Velocity

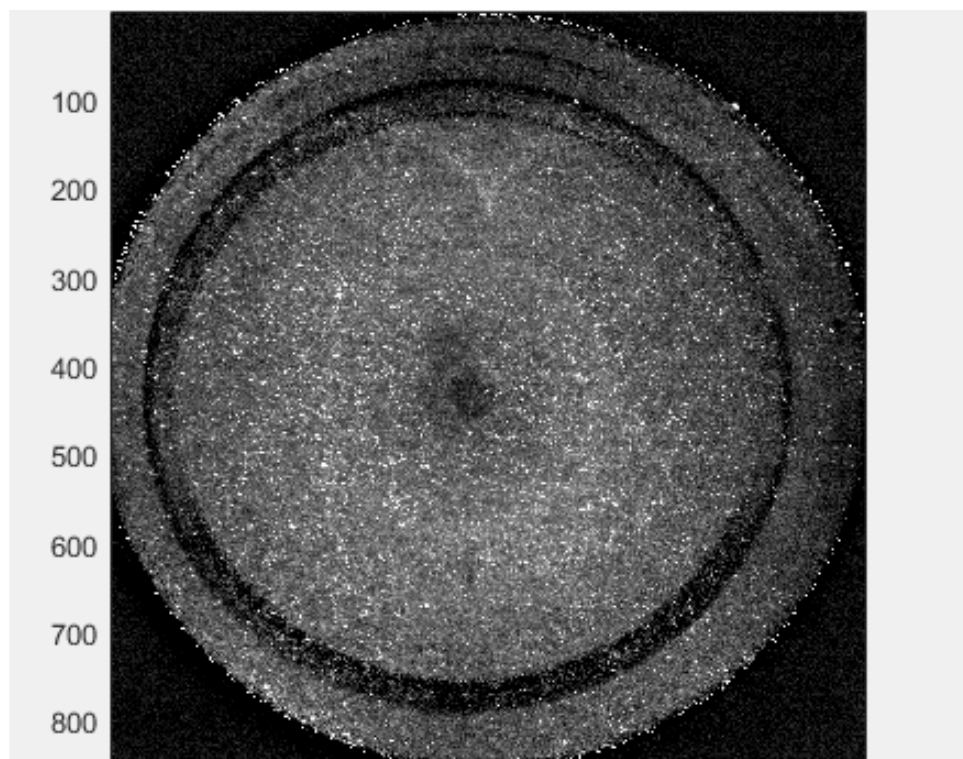


Long exposure image of a stable lean and elongated flame

- Flow structure similar to the isothermal.
- Flame anchoring within low strain rate regions

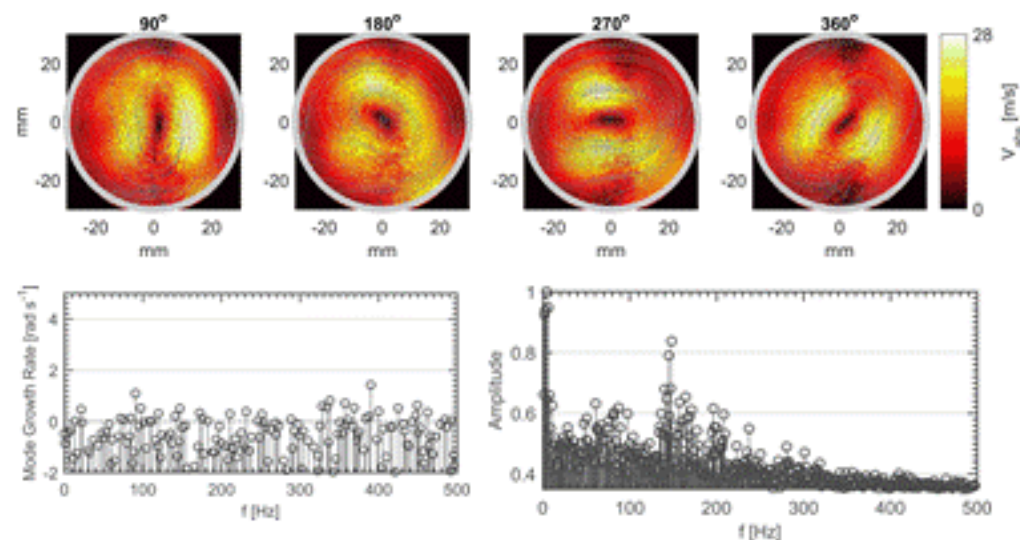


Mie Signal



DMD analysis

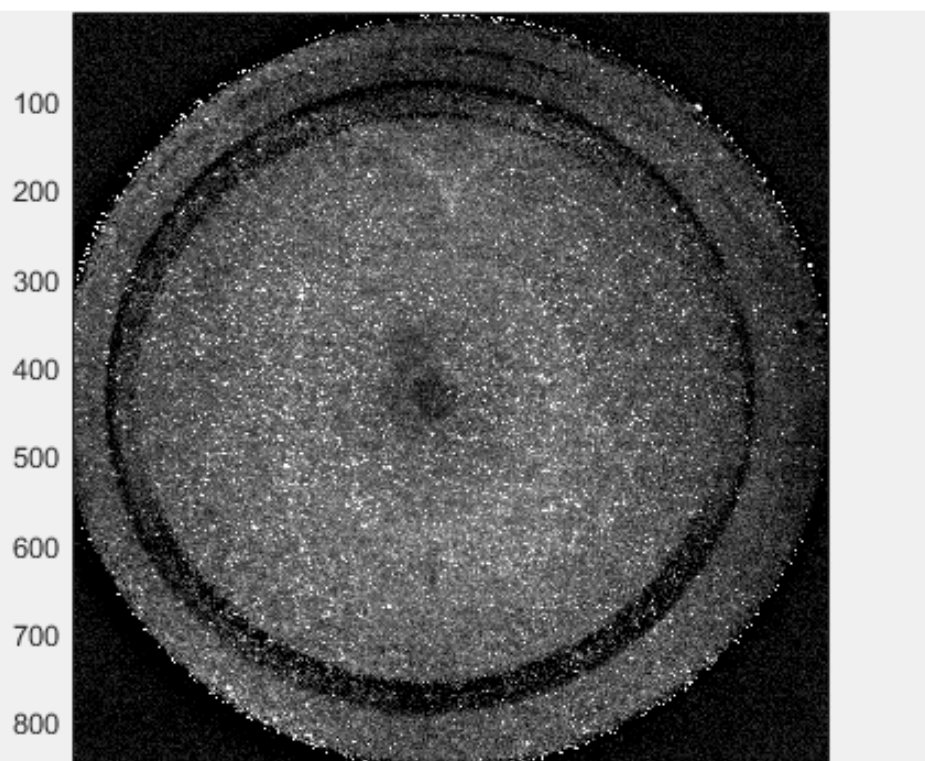
DMD Filtering at 140 Hz



DMD growth rates

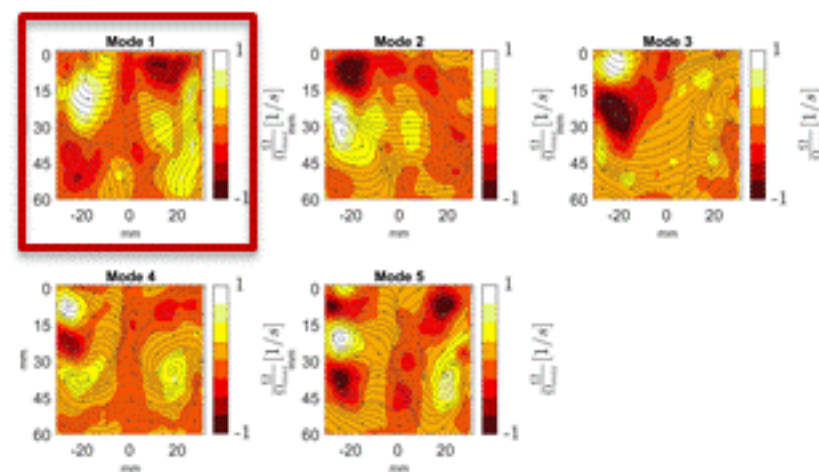
DMD amplitudes

Mie Signal

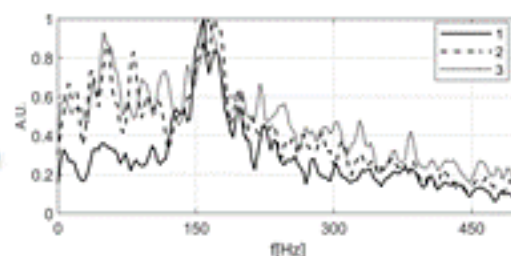


POD Modes (Normalized Vorticity)

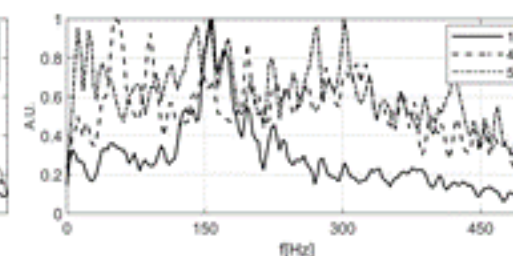
Wavemaker



POD
analysis

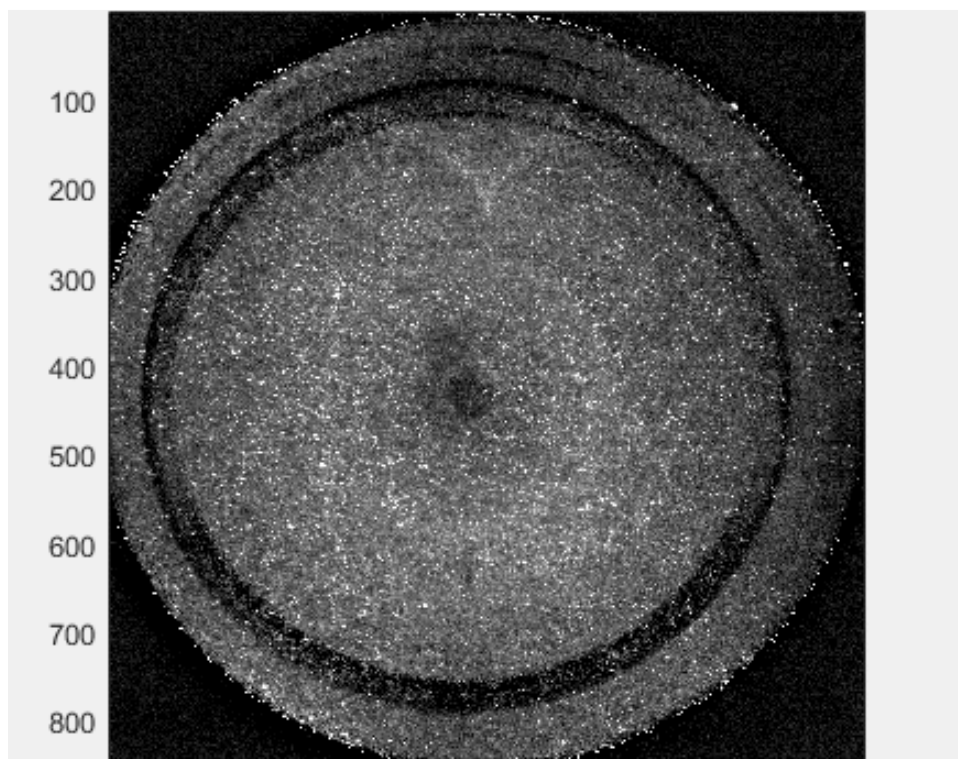


POD Spectra
Modes 1,2,3

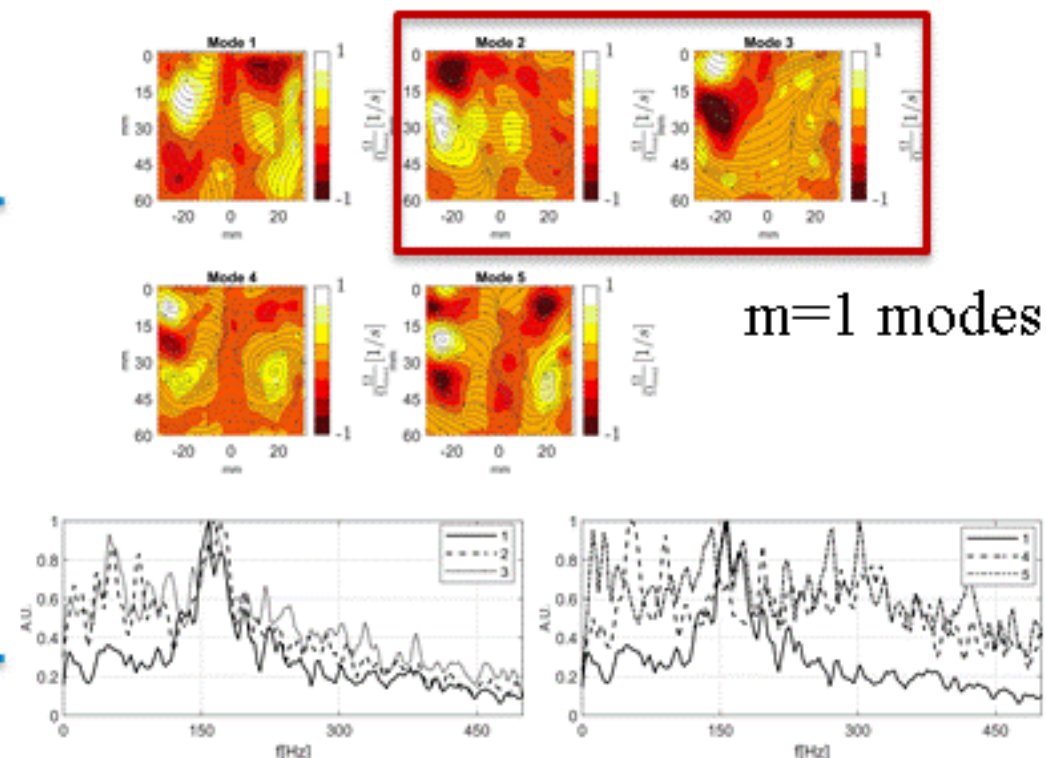


POD Spectra
Modes 1,4,5

Mie Signal



POD Modes (Normalized Vorticity)

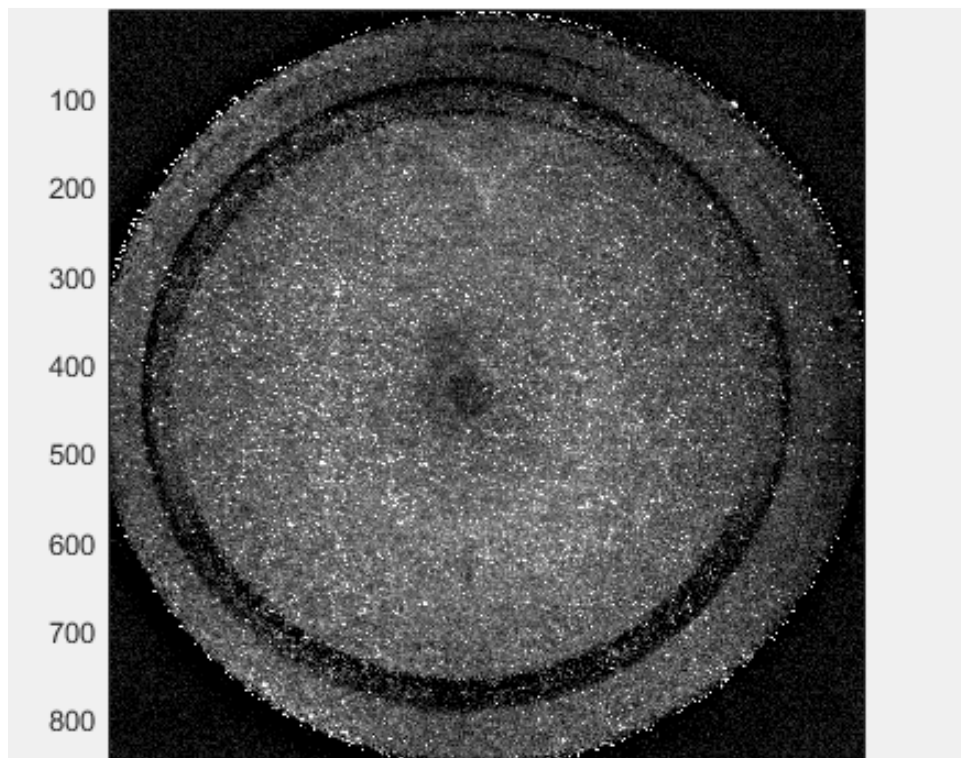


m=1 modes

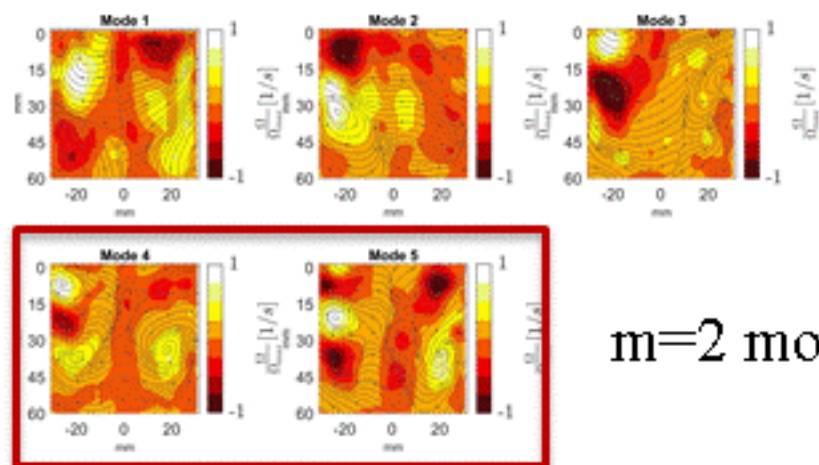
POD Spectra
Modes 1,2,3

POD Spectra
Modes 1,4,5

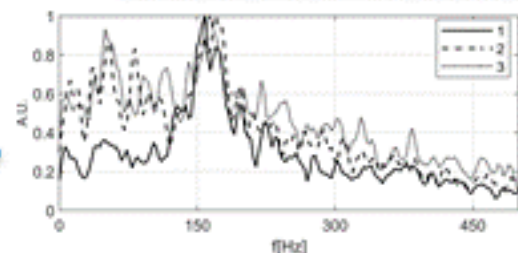
Mie Signal



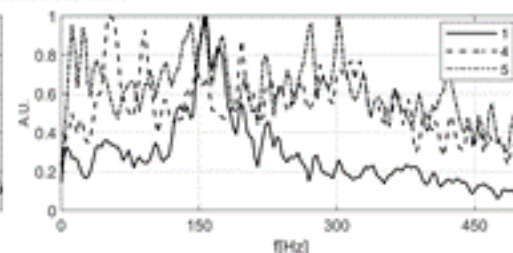
POD Modes (Normalized Vorticity)



POD
analysis



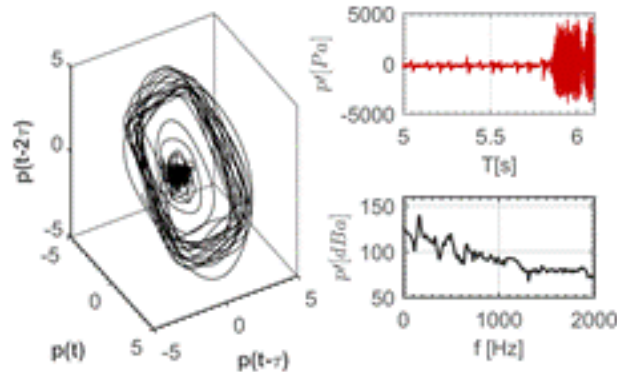
POD Spectra
Modes 1,2,3



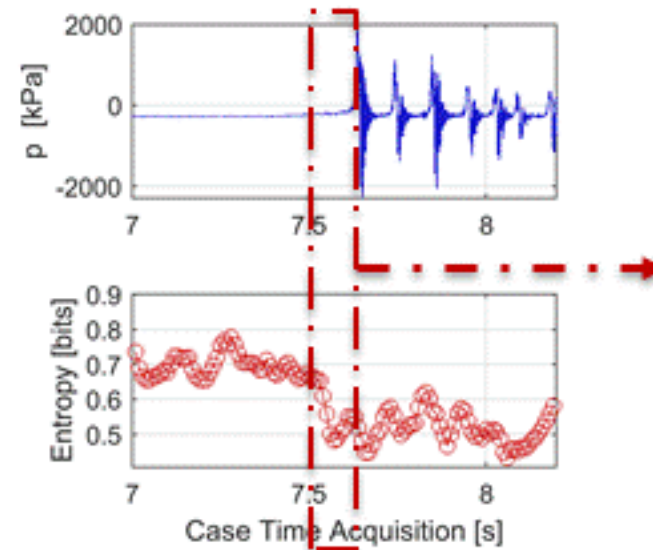
POD Spectra
Modes 1,4,5

Intermittency: Interpretation of transitional dynamics
Phase space representation

Intermittency



Permutation Entropy (forewarning method)

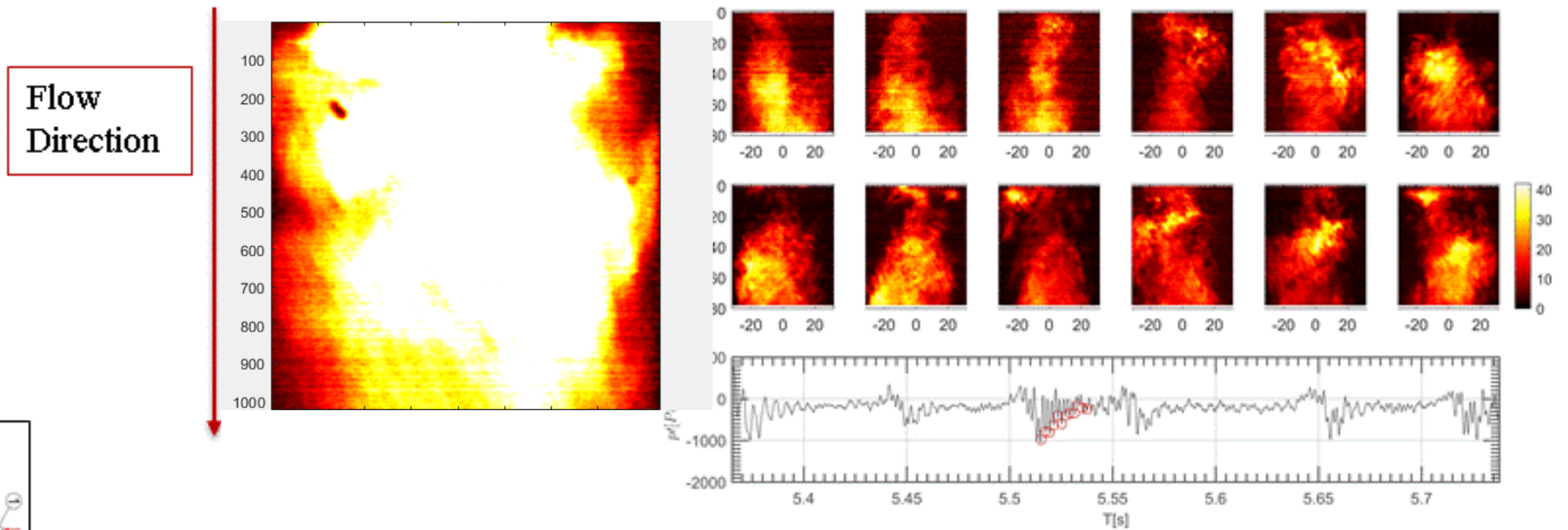


Forewarning
Period $\sim 0.15s$
 ~ 23 limit cycle
periods (160 Hz)

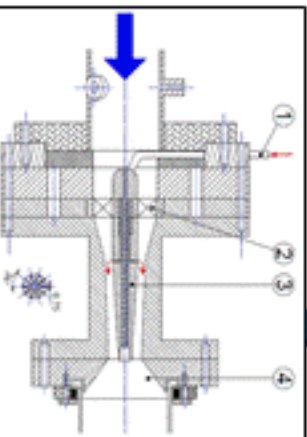
- Short term prediction techniques such as the permutation entropy were employed to trigger the PIV system and record events before the transition into Hopf bifurcation.

Flame and flowfield structure during triggering of intermittent thermoacoustic bursts

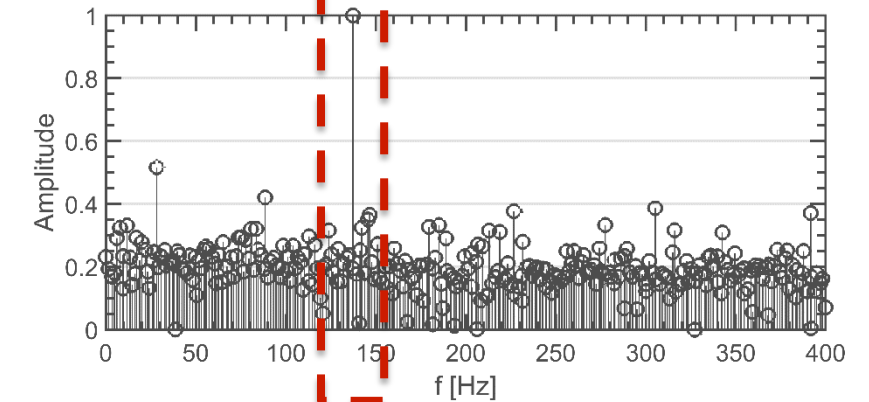
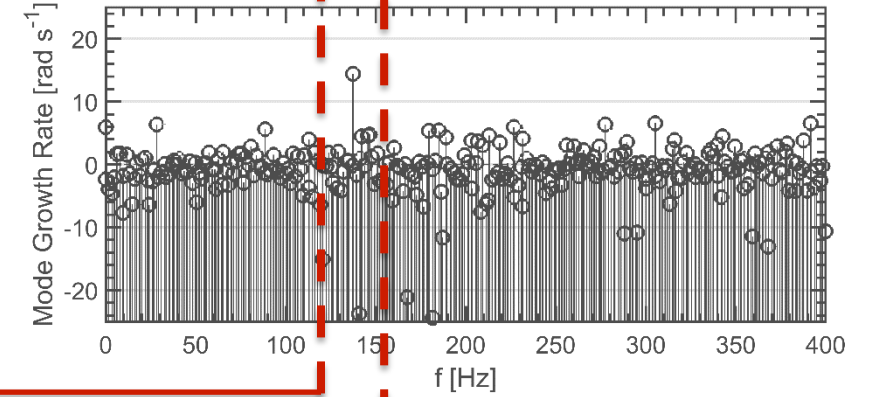
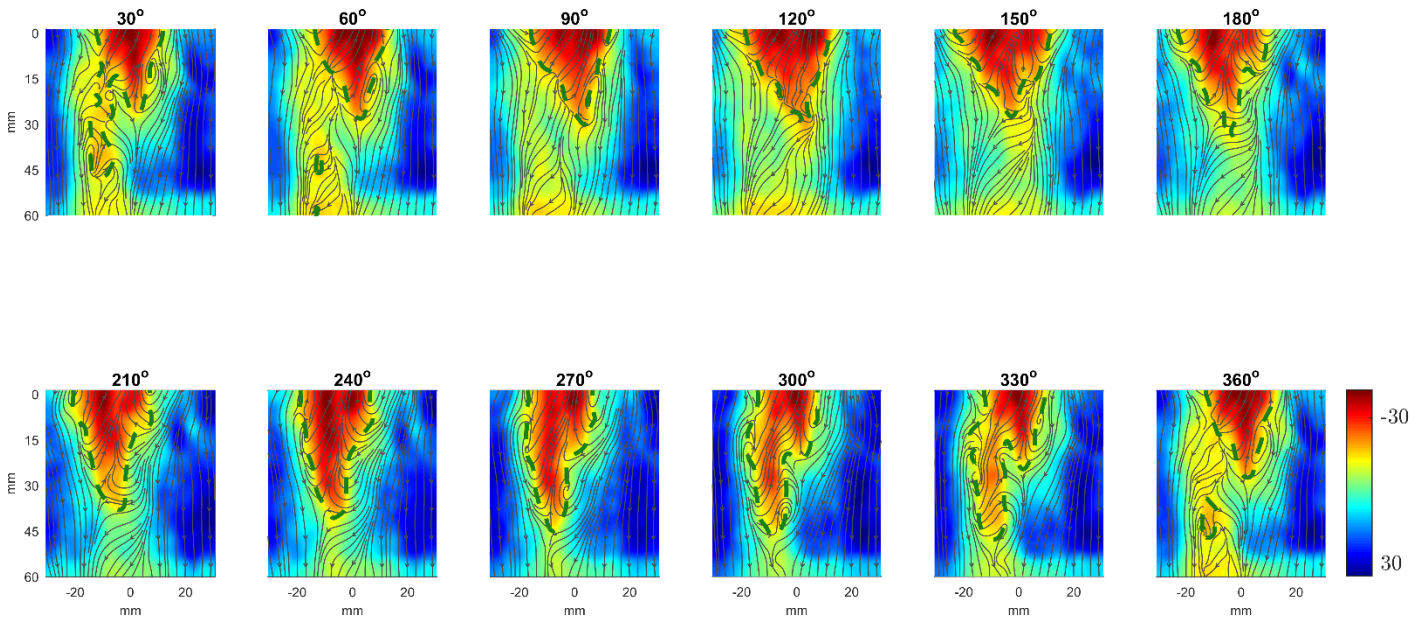
Intermittent Flame Dynamics



Dynamic pressure time series

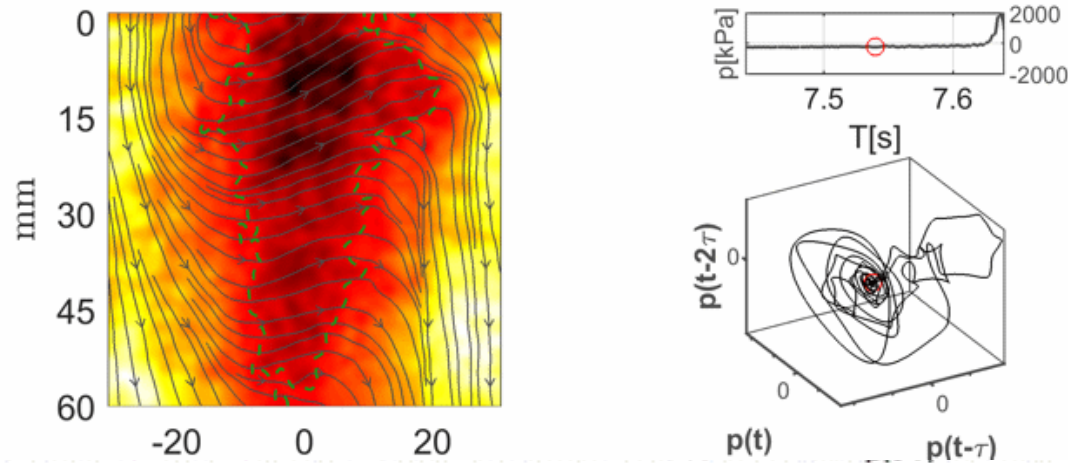


Filtering via DMD: Frequency of precession is very close to the isothermal PVC frequency of precession



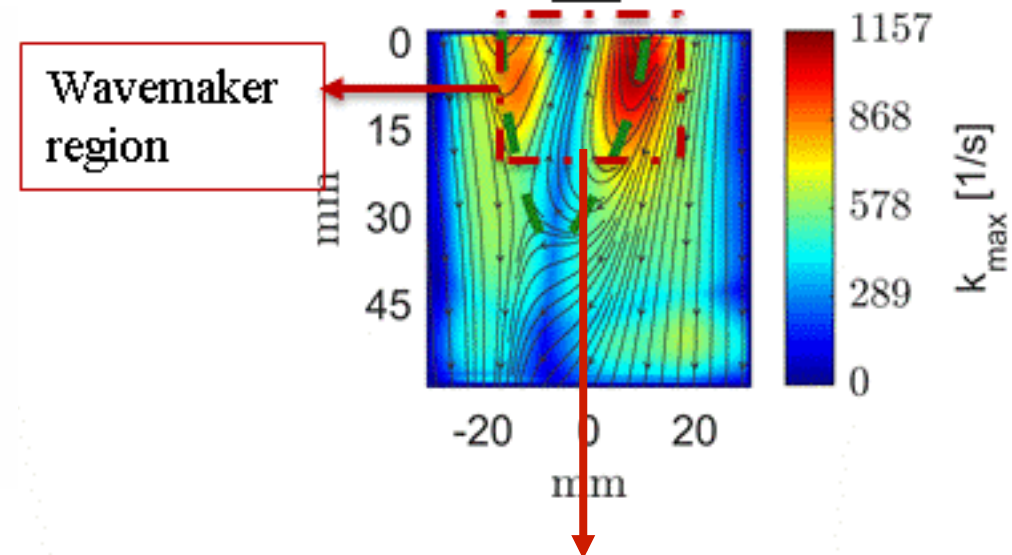
Frequency of precession: 137 Hz

Intermittent Flow Dynamics



Contours of axial velocity

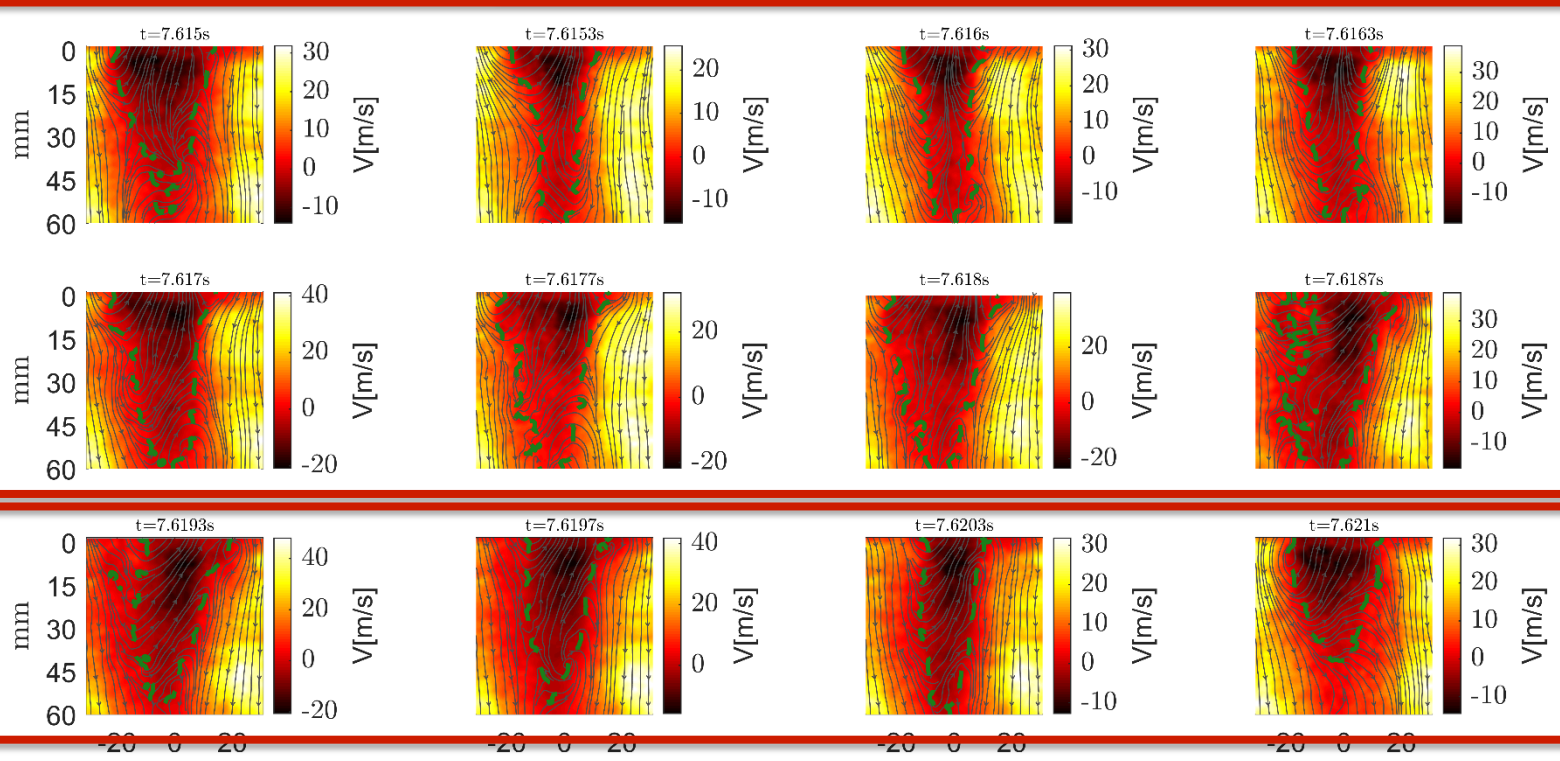
Mean strain rate (k_{flow}) during intermittency



If the elongated flame sustains straining such that it anchors close to the region wherein the helical wavemaker exists, then the flame precesses under the influence of the helical coherent structure (PVC)

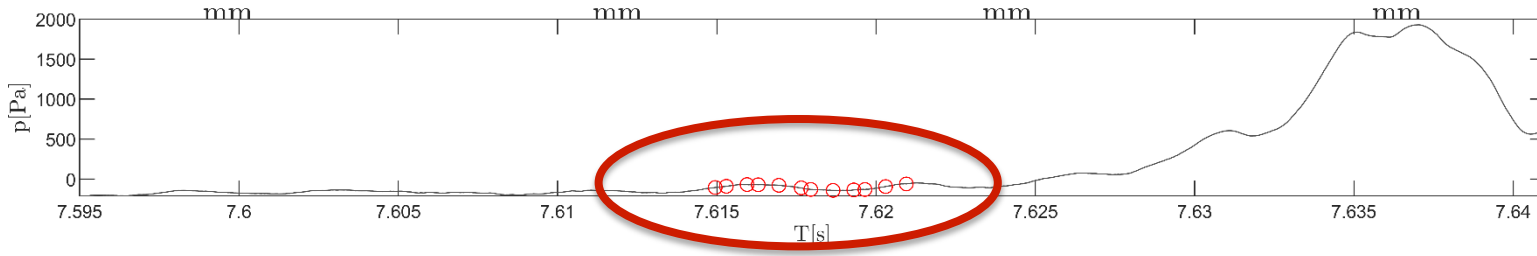
Description of dynamic state transitions

Breakdown of transition events: Pre-triggering



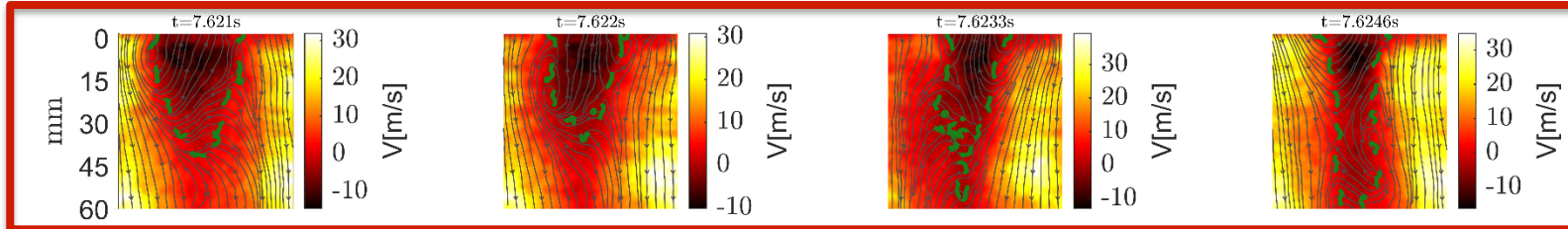
Initiation of helical motion of recirculation zone under the effect of helical coherent structures along the shear layers.

Initial formation of downstream axial stagnation point in the recirculation zone

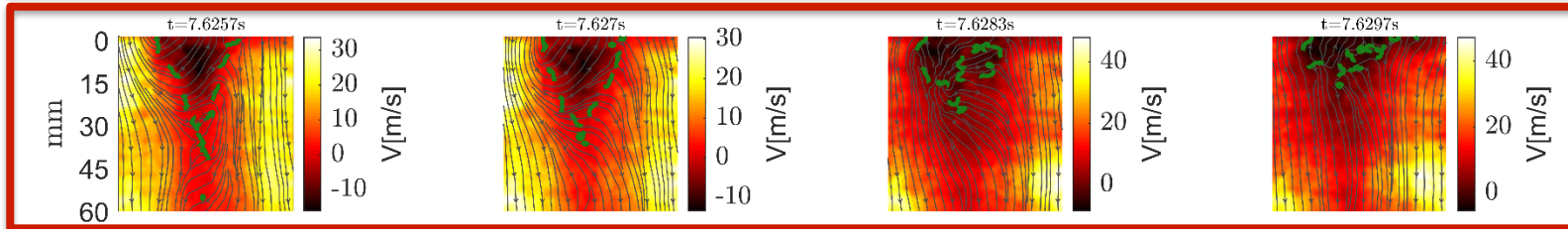


Description of dynamic state transitions

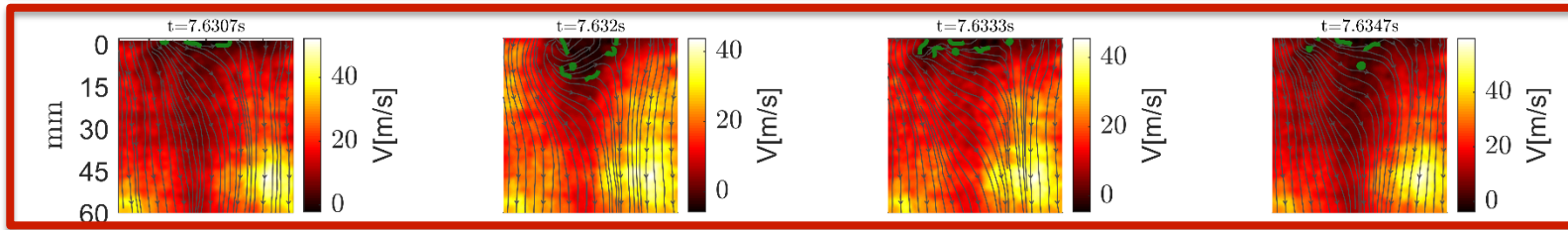
Breakdown of transition events: Thermoacoustic burst



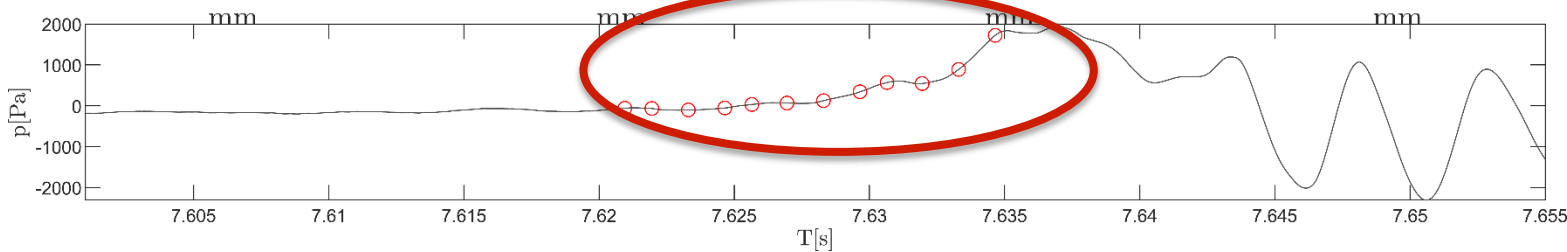
Convection of high axial velocity amplitude disturbance causing the recirculation zone to form a downstream axial stagnation point.



The passage of the disturbance decreases the axial and radial extent of the recirculation zone.

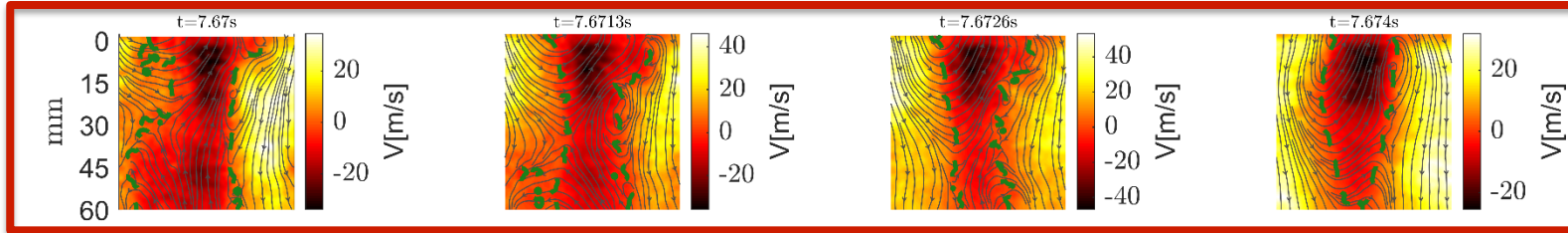


When the axial extent of the recirculation zone is minimum the dynamic pressure is maximum

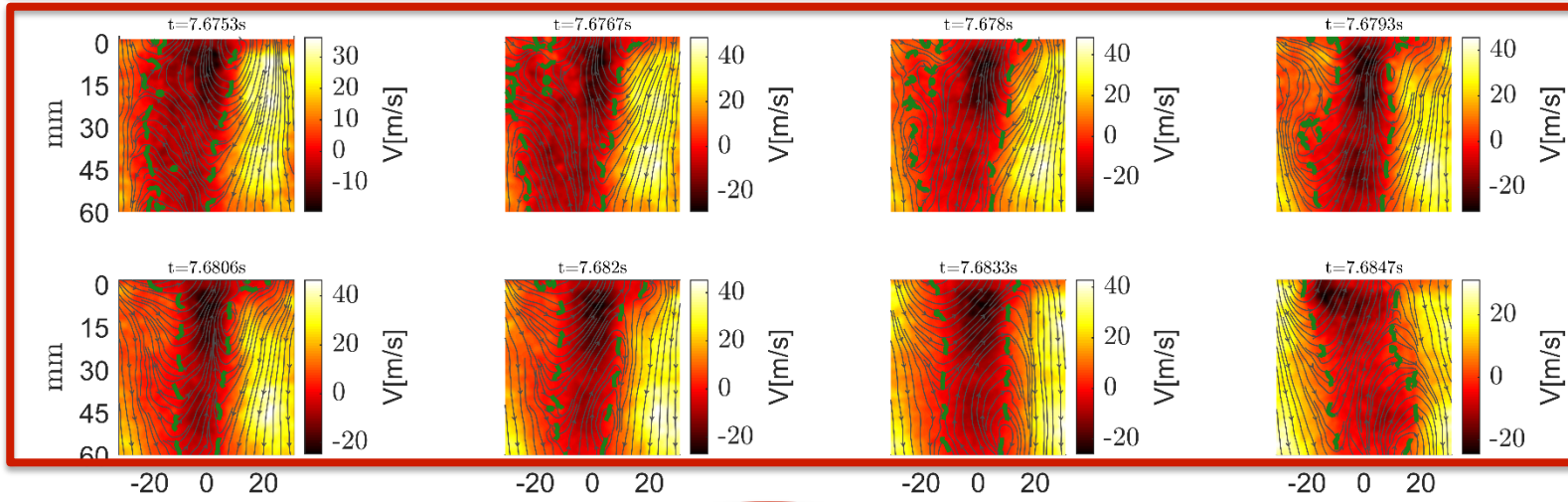


Description of dynamic state transitions

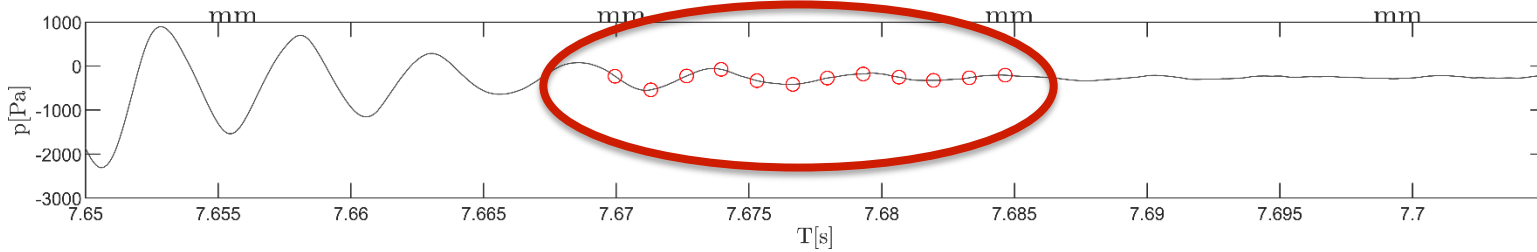
Breakdown of transition events: Requiescence



Decreasing rate of helical precession

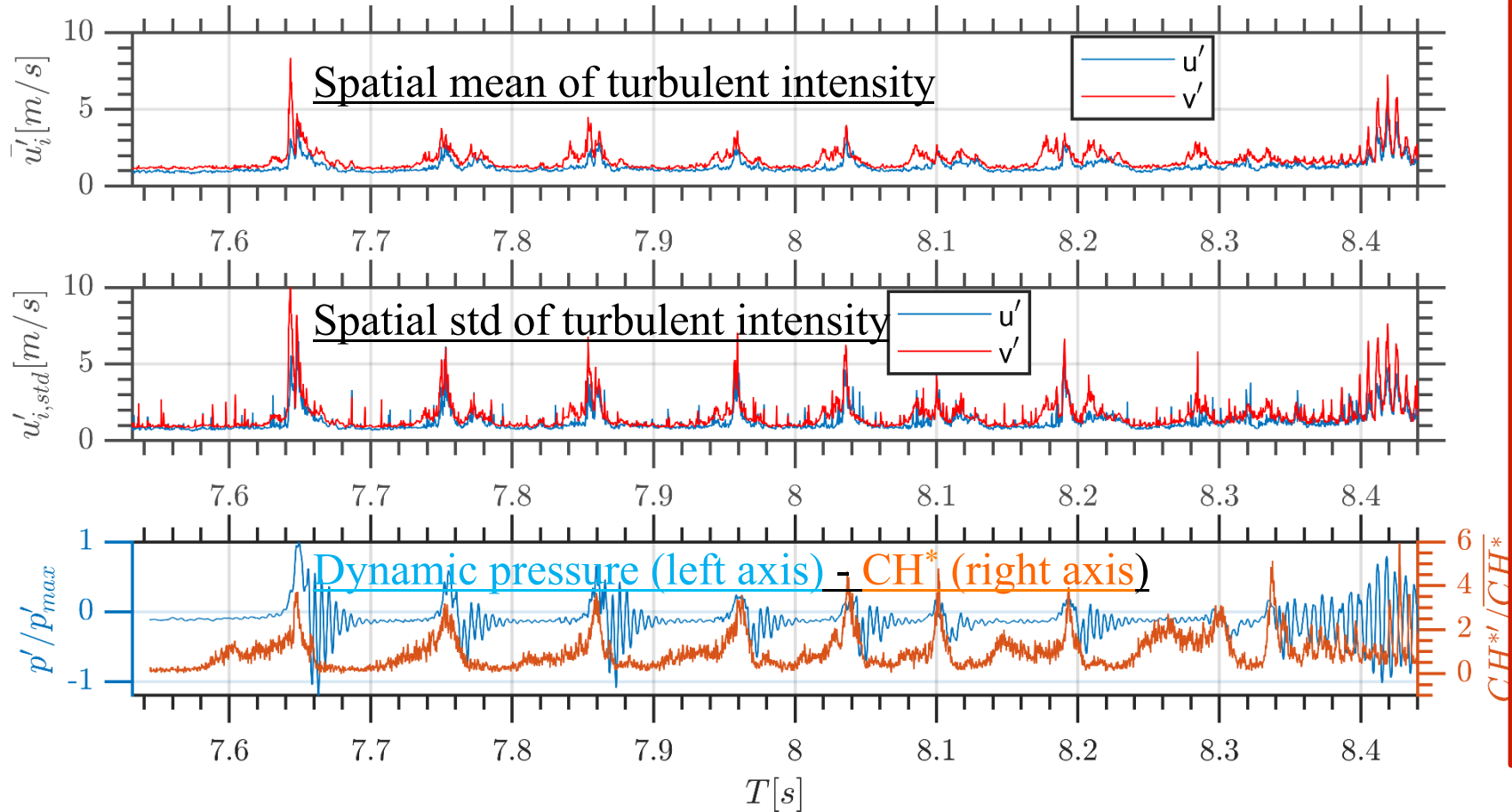


Reestablishment of open ended recirculation zone with no downstream stagnation point



Description of dynamic state transitions

Spatial mean and standard deviations of turbulent intensity

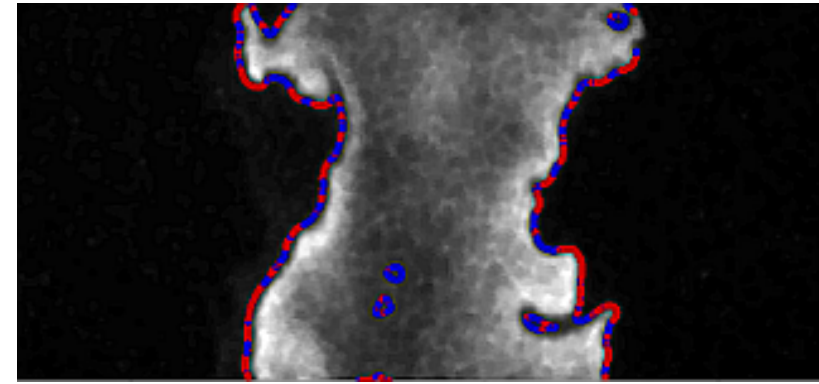
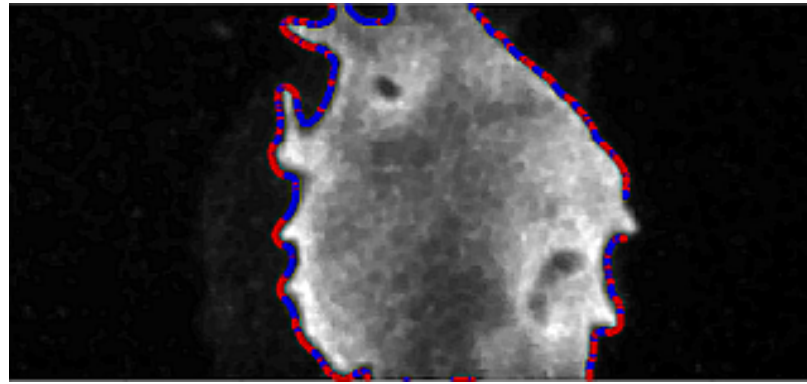
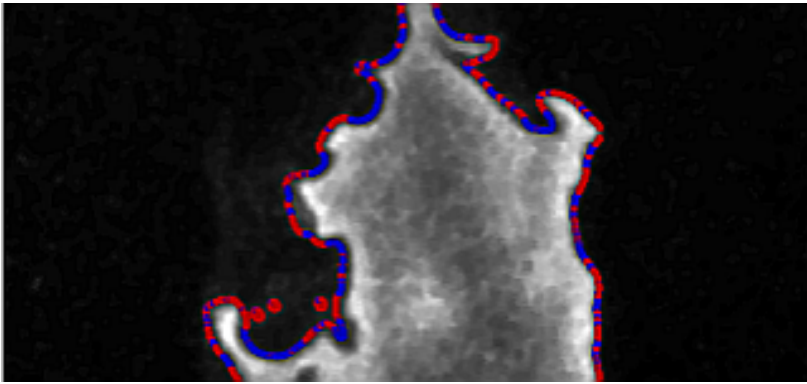


- The spatial mean and standard deviations of the turbulent intensities of the flowfield demonstrate spikes that coincide with the thermoacoustic bursts.
- The burning rate increases and the range of scales, with which the flame interacts, widens upon transitioning into thermoacoustic instability.

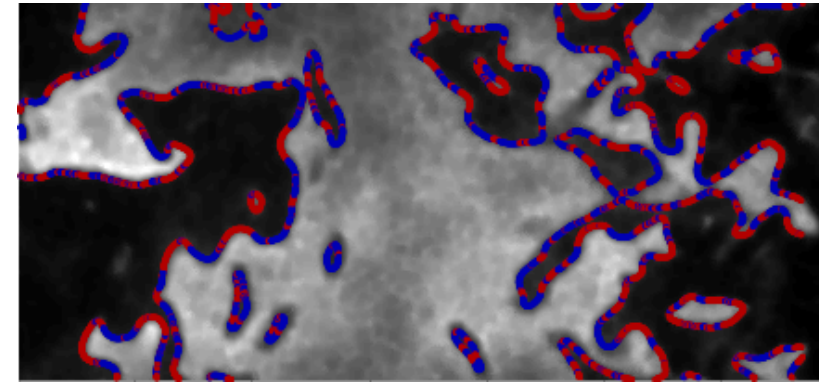
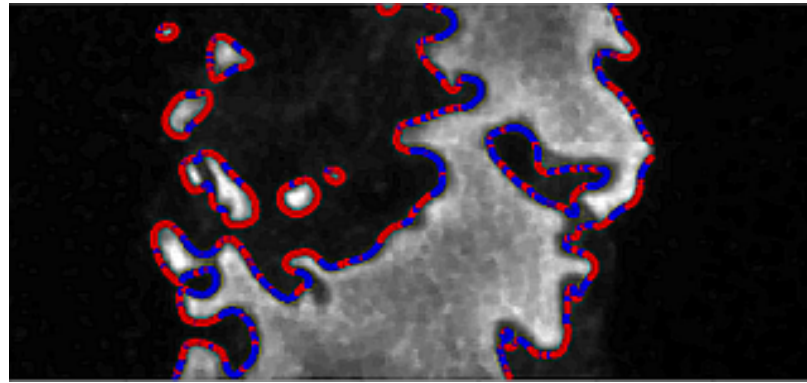
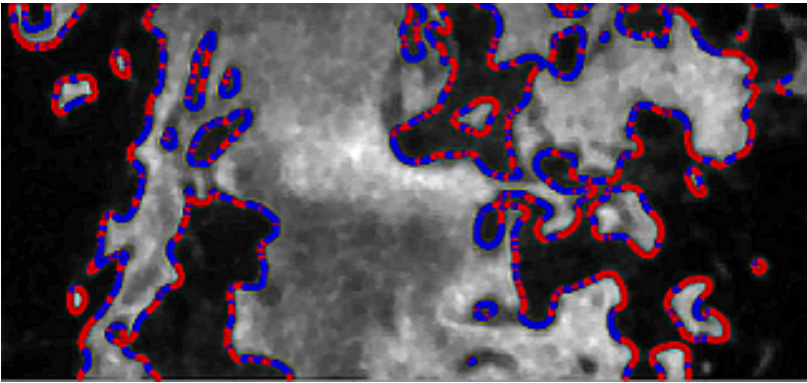
Description of dynamic state transitions

Flame front curvature characteristics of intermittent flame via OH-PLIF measurements

Quiescent flames-straight and elongated.



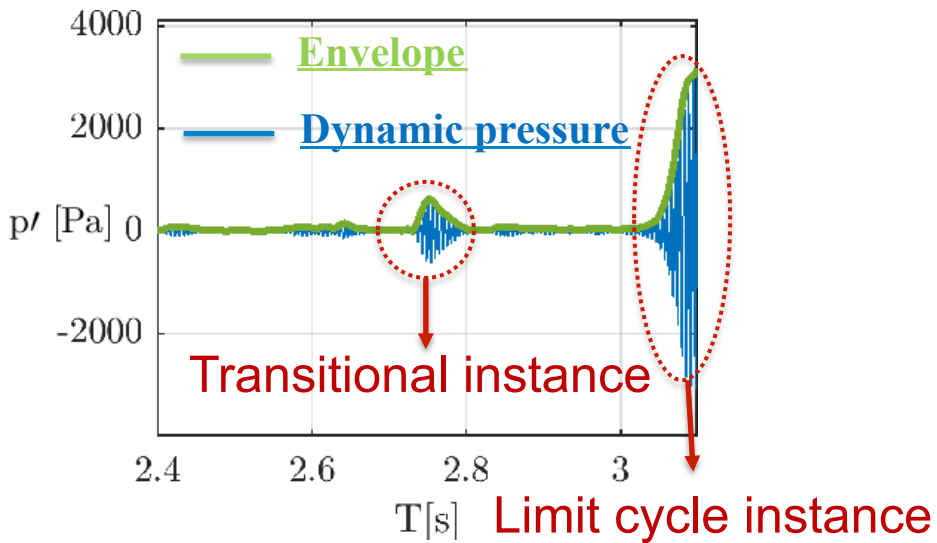
Transitional flames-more wrinkled and with greater radial extent



— Burned (Unburned
Negative curvature

Burned) Unburned +
Positive curvature

Reminder: Curvature convention



Case ID Thermoacoustic state	$\bar{\kappa}$: Mean curvature	σ : Standard deviation	μ_3 : skewness	μ_4 : kurtosis
D: Quiescent	0.115	1.108	0.091	5.045
D: Transitional	0.167	1.128	0.095	4.794
D: Limit Cycle	-0.036	1.416	-0.036	4.472
E: Quiescent	0.127	1.316	0.048	5.125
E: Transitional	0.087	1.330	0.047	4.755
E: Limit Cycle	-0.048	1.408	-0.031	4.577
F: Quiescent	0.122	1.264	0.027	5.344
F: Transitional	0.089	1.296	0.028	5.120
F: Limit Cycle	-0.024	1.402	-0.013	4.598

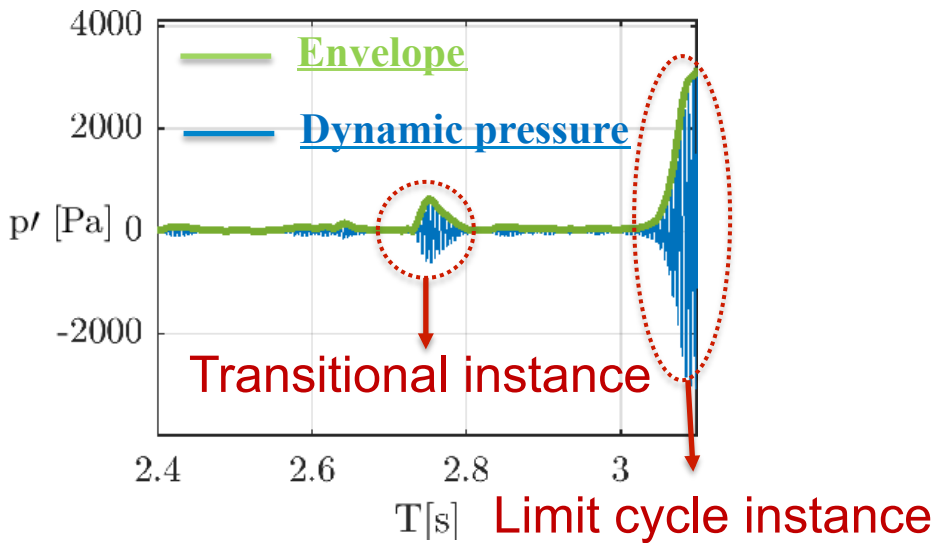
Distinction between dynamic states:

Quiescent: $p'_{\text{envelope}} < 300$ Pa

Transitional: $p'_{\text{envelope}} > 300$ Pa for at most 20 thermoacoustic cycles

Limit cycle: $p'_{\text{envelope}} > 300$ Pa for at least 20 thermoacoustic cycles

Upon transitioning from quiescence towards a limit cycle:
Mean curvature decreases towards near zero negative values



Case ID Thermoacoustic state	$\bar{\mu}$: Mean curvature	σ : Standard deviation	μ_3 : skewness	μ_4 : kurtosis
D: Quiescent	0.115	1.108	0.091	5.045
D: Transitional	0.167	1.128	0.095	4.794
D: Limit Cycle	-0.036	1.416	-0.036	4.472
E : Quiescent	0.127	1.316	0.048	5.125
E: Transitional	0.087	1.330	0.047	4.755
E: Limit Cycle	-0.048	1.408	-0.031	4.577
F: Quiescent	0.122	1.264	0.027	5.344
F: Transitional	0.089	1.296	0.028	5.120
F: Limit Cycle	-0.024	1.402	-0.013	4.598

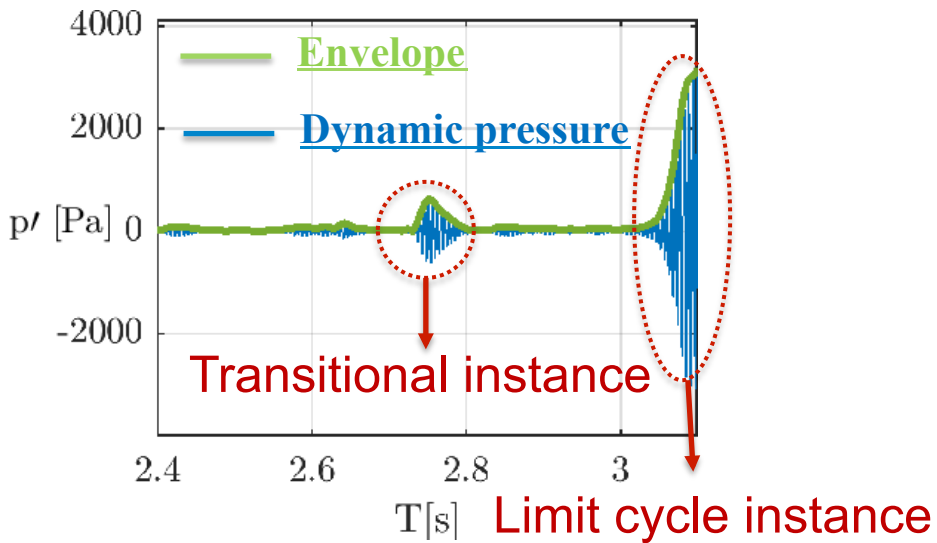
Distinction between dynamic states:

Quiescent: $p'_{\text{envelope}} < 300$ Pa

Transitional: $p'_{\text{envelope}} > 300$ Pa for at most 20 thermoacoustic cycles

Limit cycle: $p'_{\text{envelope}} > 300$ Pa for at least 20 thermoacoustic cycles

Upon transitioning from quiescence towards a limit cycle:
Standard deviation strongly increases.



Case ID Thermoacoustic state	$\bar{\mu}$: Mean curvature	σ : Standard deviation	μ_3 : skewness	μ_4 : kurtosis
D: Quiescent	0.115	1.108	0.091	5.045
D: Transitional	0.167	1.128	0.095	4.794
D: Limit Cycle	-0.036	1.416	-0.036	4.472
E: Quiescent	0.127	1.316	0.048	5.125
E: Transitional	0.087	1.330	0.047	4.755
E: Limit Cycle	-0.048	1.408	-0.031	4.577
F: Quiescent	0.122	1.264	0.027	5.344
F: Transitional	0.089	1.296	0.028	5.120
F: Limit Cycle	-0.024	1.402	-0.013	4.598

Distinction between dynamic states:

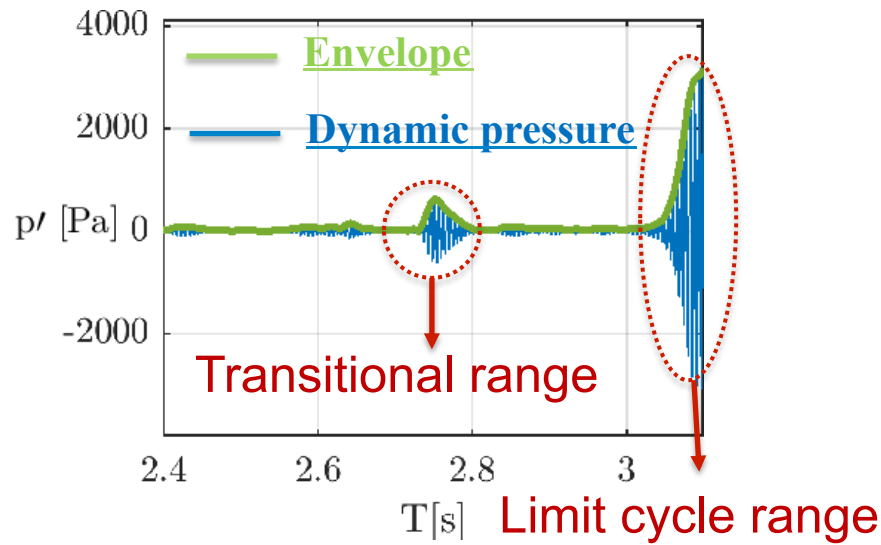
Quiescent: $p'_{\text{envelope}} < 300$ Pa

Transitional: $p'_{\text{envelope}} > 300$ Pa for at most 20 thermoacoustic cycles

Limit cycle: $p'_{\text{envelope}} > 300$ Pa for at least 20 thermoacoustic cycles

Upon transitioning from quiescence towards a limit cycle:
Standard deviation strongly increases.

Upon transitioning from quiescence towards a limit cycle:
Kurtosis decreases



Case ID Thermoacoustic state	$\bar{\mu}$: Mean curvature	σ : Standard deviation	μ_3 : skewness	μ_4 : kurtosis
D: Quiescent	0.115	1.108	0.091	5.045
D: Transitional	0.167	1.128	0.095	4.794
D: Limit Cycle	-0.036	1.416	-0.036	4.472
E: Quiescent	0.127	1.316	0.048	5.125
E: Transitional	0.087	1.330	0.047	4.755
E: Limit Cycle	-0.048	1.408	-0.031	4.577
F: Quiescent	0.122	1.264	0.027	5.344
F: Transitional	0.089	1.296	0.028	5.120
F: Limit Cycle	-0.024	1.402	-0.013	4.598

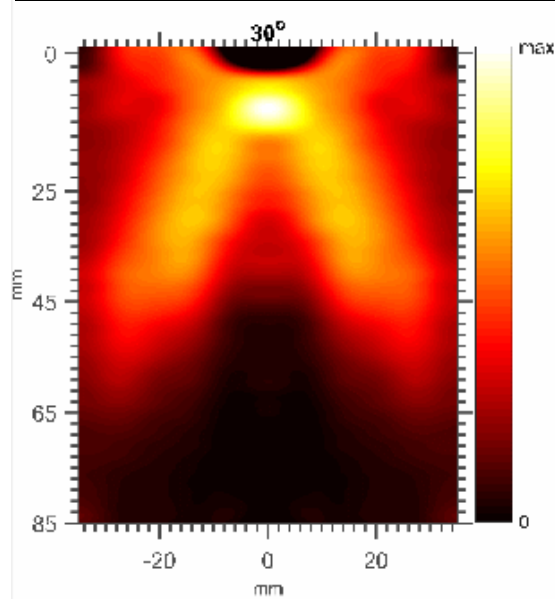
Distinction between dynamic states:
Quiescent: $p'_{\text{envelope}} < 300$ Pa
Transitional: $p'_{\text{envelope}} > 300$ Pa for at most 20 thermoacoustic cycles
Limit cycle: $p'_{\text{envelope}} > 300$ Pa for at least 20 thermoacoustic cycles

Flames that experience subcritical Hopf bifurcations gradually become more wrinkled while transitioning through the transitional thermoacoustic state towards the limit cycle.

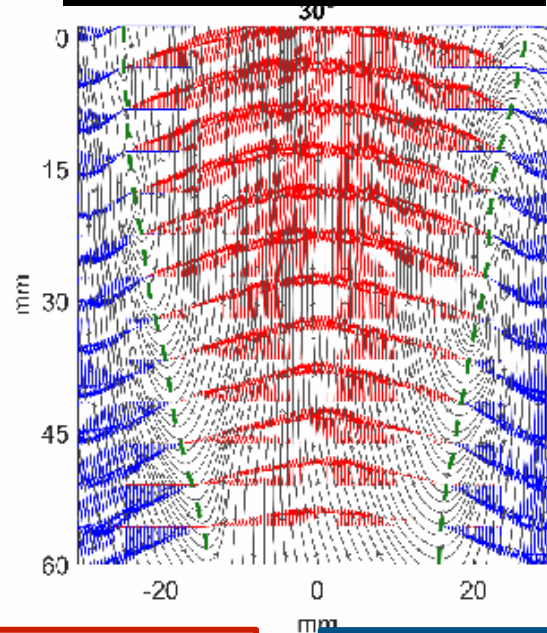
Interpretation of limit cycle perpetuation mechanism

Limit Cycle structure Case G (60% CH₄ – 40% H₂)

CH* high speed imaging



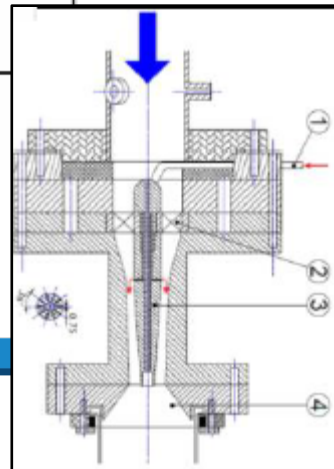
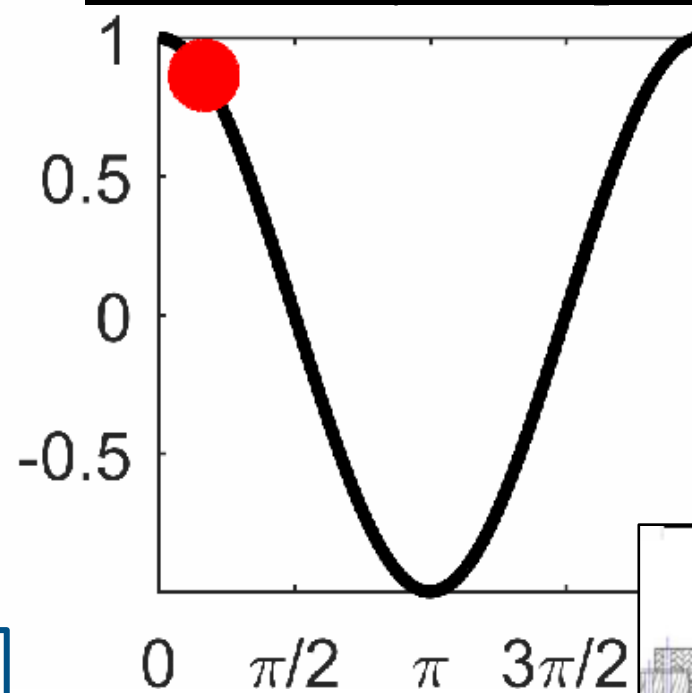
PIV measurements



Recirculation
Zone

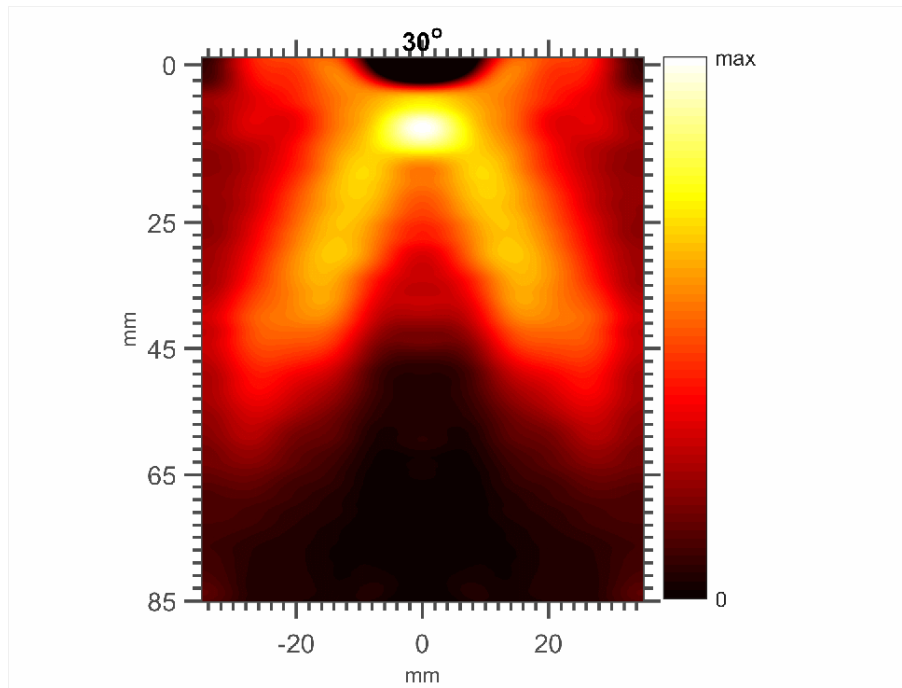
Free Stream
Velocity

Indicative dynamic pressure trace

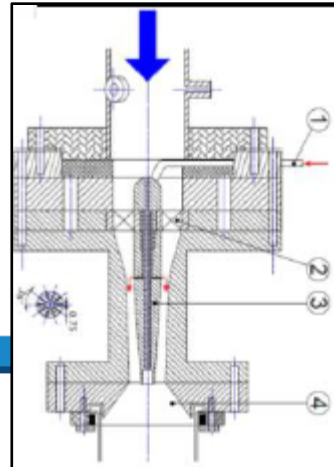
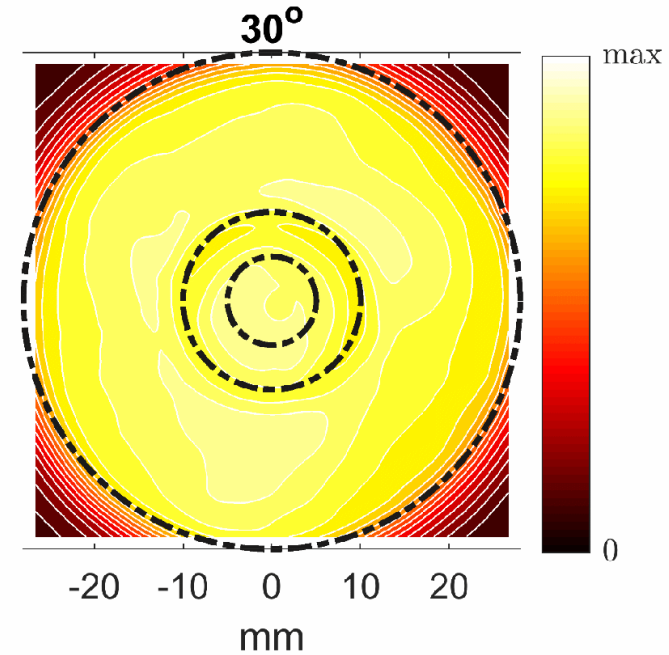


Limit Cycle structure Case G (60% CH₄ – 40% H₂)

CH* axial-radial



CH* azimuthal-radial

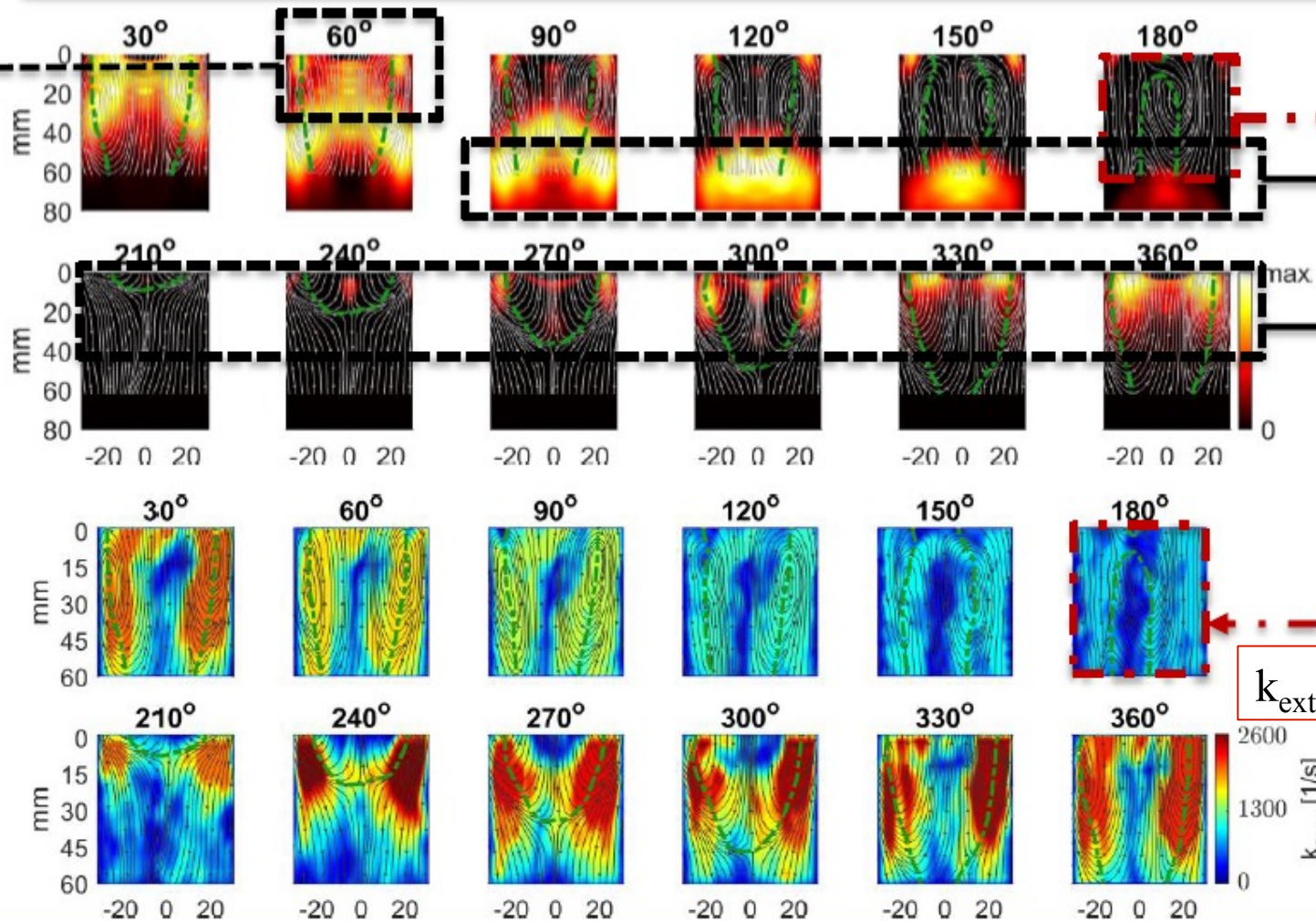


Limit Cycle structure Cage G (60% CH₄ – 40% H₂)

Initiation of
local extinction

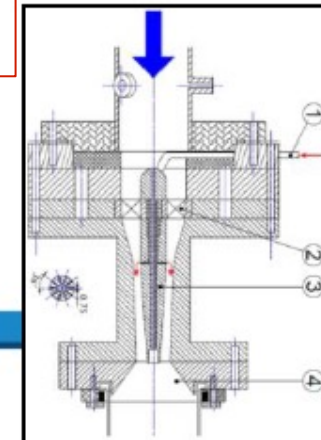
Phase averaged
 I_{CH}^*

Phase averaged
strain rate (k_{flow})



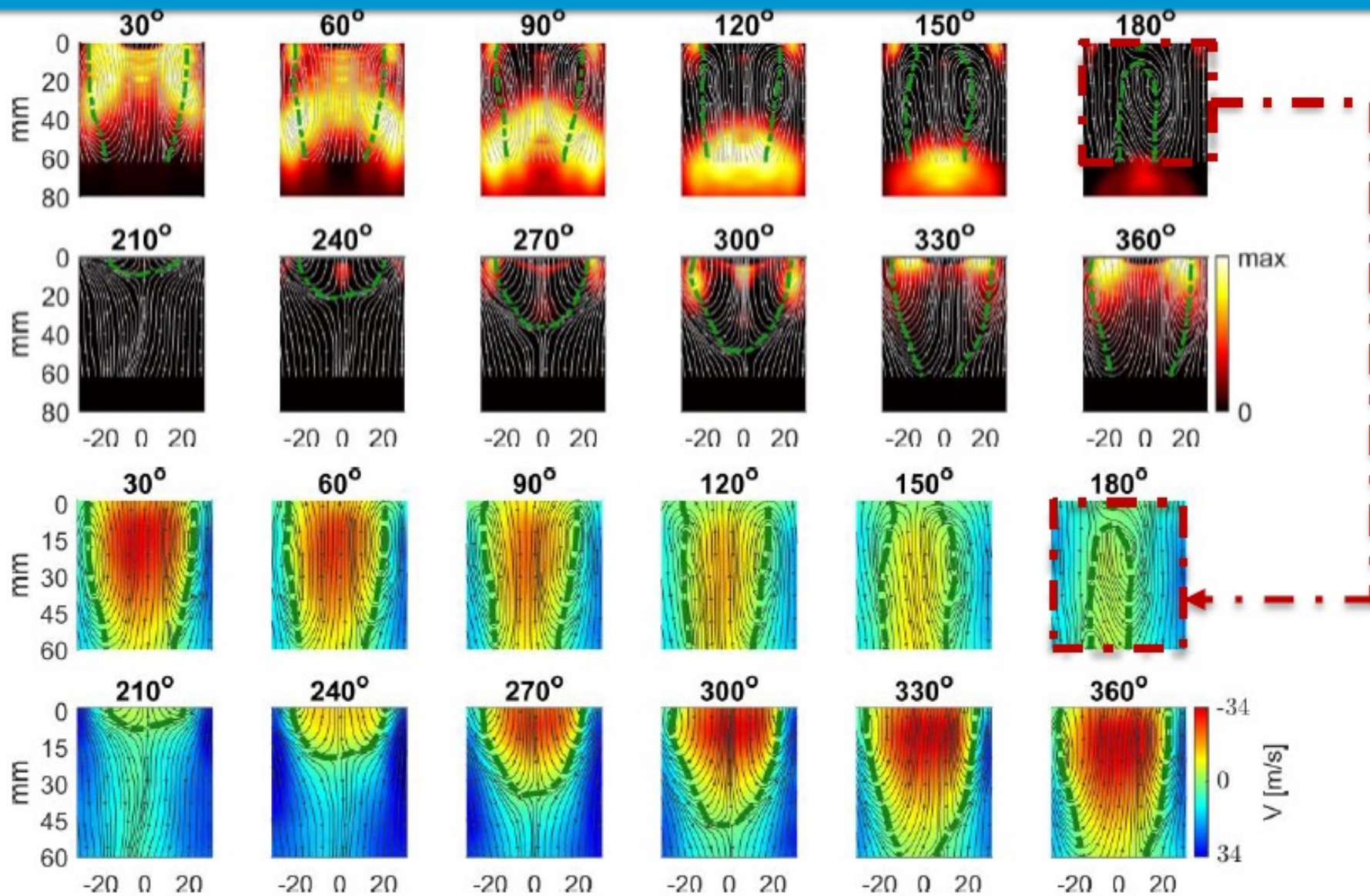
Convection of
residual flame
the mean flow

Flame propagating
along inner shear
layers



Limit Cycle structure Case G (60% CH₄ – 40% H₂)

Phase averaged
flame structure



Phase averaged
axial velocity

Summary: During a subcritical Hopf bifurcation, how does the flame and flowfield structure bifurcate?

- Intermittency is observed when the flame is able to penetrate and anchor in the “Wavemaker” region, close to the inlet of the burner. To do so the flame needs to overcome increased strain rates in this region of the flowfield.
- Flames tolerant to extinction strain rates are more susceptible to demonstrating subcritical Hopf bifurcations.
- Transition into instability in the model gas turbine combustor is associated with:
 1. the PVC which imposes helical disturbances on the flame and the recirculation zone.
 2. Loss of randomness in the dynamic state: employed to forewarn of triggering.
- The role of the PVC is crucial. It exists both for the isothermal and the quiescent flowfields and it can instigate thermoacoustic bursts that are promoted mainly by the flame-wall interactions.

Summary: During a subcritical Hopf bifurcation, how do the flame and flowfield structure bifurcate?

- The flames of thermoacoustic systems demonstrating subcritical Hopf bifurcations assume increasingly wrinkled states. This is supported by both PIV and PLIF measurements:
 1. The standard deviation of the turbulent intensities during the transition into thermoacoustic instability increases.
 2. The standard deviation and the kurtosis of the flame front curvature increase.
- The extinction strain rate plays an important role in the perpetuation of limit cycle thermoacoustic oscillations as well. It leads to successive extinction-reignition of the flame thus perpetuating the limit cycle.